



**HAL**  
open science

# Quantitative Measurement of Rare Earth Elements in Brines: Isolation from the Charged Matrix Versus Direct LA-ICP-MS Measurements – A Comparative Study

Maria A Kokh, Béatrice Luais, Laurent Truche, Marie Christine Boiron,  
Chantal Peiffert, Aimeryc Schumacher

## ► To cite this version:

Maria A Kokh, Béatrice Luais, Laurent Truche, Marie Christine Boiron, Chantal Peiffert, et al.. Quantitative Measurement of Rare Earth Elements in Brines: Isolation from the Charged Matrix Versus Direct LA-ICP-MS Measurements – A Comparative Study. *Geostandards and Geoanalytical Research*, 2021, 45 (2), pp.341-358. 10.1111/GGR.12376 . hal-03360101

**HAL Id: hal-03360101**

**<https://hal.univ-lorraine.fr/hal-03360101>**

Submitted on 30 Sep 2021

**HAL** is a multi-disciplinary open access archive for the deposit and dissemination of scientific research documents, whether they are published or not. The documents may come from teaching and research institutions in France or abroad, or from public or private research centers.

L'archive ouverte pluridisciplinaire **HAL**, est destinée au dépôt et à la diffusion de documents scientifiques de niveau recherche, publiés ou non, émanant des établissements d'enseignement et de recherche français ou étrangers, des laboratoires publics ou privés.

1 **Quantitative Measurement of Rare Earth Elements in Brines: Isolation from the**  
2 **Charged Matrix Versus Direct LA-ICP-MS Measurements, a Comparative Study**

3  
4 **Maria A. Kokh<sup>a,b,\*</sup>, Béatrice Luais<sup>c</sup>, Laurent Truche<sup>b</sup>, Marie Christine Boiron<sup>a</sup>,**  
5 **Chantal Peiffert<sup>a</sup> and Aimeryc Schumacher<sup>c</sup>**

6  
7 <sup>a</sup> Université de Lorraine, CNRS, GeoRessources, F-54000 Nancy, France

8 [marie-christine.boiron@univ-lorraine.fr](mailto:marie-christine.boiron@univ-lorraine.fr), [chantal.peiffert@univ-lorraine.fr](mailto:chantal.peiffert@univ-lorraine.fr)

9 <sup>b</sup> Institut des Sciences de la Terre (ISTerre) - UMR 5275 of CNRS, Université Grenoble Alpes, 1381

10 rue de la Piscine, B.P. 53, 38041 Grenoble, France [laurent.truche@univ-grenoble-alpes.fr](mailto:laurent.truche@univ-grenoble-alpes.fr)

11 <sup>c</sup> Université de Lorraine, CNRS, CRPG, F-54000 Nancy, France [luais@crpg.cnrs-nancy.fr](mailto:luais@crpg.cnrs-nancy.fr),

12 [aimeryc@crpg.cnrs-nancy.fr](mailto:aimeryc@crpg.cnrs-nancy.fr)

13 \* Present address: Universität Potsdam, Institut für Geowissenschaften, Campus Golm, Haus 27,

14 Karl-Liebknecht-Str. 24-25, 14476 Potsdam, Germany [kokh@uni-potsdam.de](mailto:kokh@uni-potsdam.de)

15  
16 Corresponding author: [laurent.truche@univ-grenoble-alpes.fr](mailto:laurent.truche@univ-grenoble-alpes.fr)

17  
18  
19  
20  
21  
22  
23 Revised version 12/01/2021

## Abstract

24  
25  
26 The quantification of the REEs in natural rocks and fluids is important not only for the  
27 sustainable use of geological resources but also for fundamental geological research. Due to  
28 significant improvements in experimental, modeling and analytical techniques, it was  
29 discovered that the REEs could be efficiently mobilized and transported by hydrothermal fluids.  
30 Thus, analyzing the REEs in fluids, especially in highly saline solutions, is a prerequisite to  
31 understand their fate in hydrothermal fluids. An analytical methodology was established to  
32 determine the trace quantities of the REEs in aqueous solutions with compositions typical to  
33 seawater and brines. The developed protocol was applied for the REEs quantification in  
34 experimental sodium-rich carbonate-bearing hydrothermal solutions. For this purpose, we used  
35 two analytical approaches: i) the REEs were chromatographically isolated from the charged  
36 matrix and introduced in a single collector quadrupole ICP-MS, and ii) direct analysis of the REEs  
37 by LA-ICP-MS contents of experimental solutions loaded into glass capillaries without any  
38 additional isolation procedure. Both LA-ICP-MS and solution nebulization ICP-MS analysis after  
39 the REEs isolation provide identic data in terms of the REEs concentrations in brines and are  
40 consistent within analytical uncertainties. Being an express method, LA-ICP-MS could be  
41 recommended for the REEs quantification in brines. At the same time, the REEs' isolation from  
42 the charged matrix with subsequent ICP-MS analysis provides higher accuracy and precision,  
43 giving additional information for the REEs mass fractions that are below the detection limit of  
44 the LA-ICP-MS that was estimated at  $\sim 10 \text{ ng g}^{-1}$  level.

45

46 **Keywords:** rare earth elements, brine, cation-exchange resin, ICP-MS, LA-ICP-MS.

47

48 **1. Introduction**

49

50 **Geological and industrial significance of precise quantification of the rare earth elements in**  
51 **hydrothermal brines**

52

53 The rare earth elements (REEs) are crucial in many modern technologies, such as  
54 mobile phones, screens, hard drives, electric vehicles, and play a key role in the development of  
55 techniques related to the renewable carbon-free energy industry. The rise of demand for many  
56 items that require rare earth metals induced an increase in metal mining and stimulated  
57 significant industrial efforts for their efficient recovery and recycling, as well as prospection of  
58 new deposits. The quantification of the REEs in natural rocks and fluids is important not only for  
59 the sustainable use of natural resources but also for the fundamental geological research: the  
60 rare earths are widely used as redox conditions proxies (*e.g.*, [Bau 1991](#), [González-Álvarez and](#)  
61 [Kerrick 2010](#)), geothermobarometers (*e.g.*, [Gratz and Heinrich 1998](#), [Heinrich \*et al.\* 1997](#), [Pyle](#)  
62 [\*et al.\* 2001](#)), geochronometers using the  $^{147}\text{Sm}$ - $^{143}\text{Nd}$  and  $^{146}\text{Sm}$ - $^{142}\text{Nd}$  (*e.g.*, [Workman and Hart](#)  
63 [2005](#), [Boyet and Carlson 2006](#)),  $^{138}\text{La}$ - $^{138}\text{Ce}$  ([Tanaka and Masuda 1982](#)) systems, and  
64 geochemical tracers of various petrogenetic processes occurring in mantle, crust and seafloor  
65 hydrothermal systems (*e.g.*, [Luais \*et al.\* 2009](#), [Schmidt \*et al.\* 2010](#), [Cole \*et al.\* 2014](#), [Mercadier \*et\*](#)  
66 [\*al.\* 2011](#), [Doucelance \*et al.\* 2014](#), [Chavagnac \*et al.\* 2018](#)).

67 For a long time, magmatism and sedimentary processes were considered as two main  
68 forces controlling the distribution of the REEs on the Earth. However, during the last thirty  
69 years, due to significant improvements in experimental, modeling and analytical techniques  
70 (*e.g.*, [Wood 1990](#), [Bau 1991](#), [Ghazy \*et al.\* 1993](#)), it was found that the REEs could be efficiently  
71 mobilized and transported by hydrothermal fluids as a result of both regional or contact

72 metamorphism (*e.g.*, [González-Álvarez and Kerrich 2010](#), [Richard \*et al.\* 2013](#)) and post-  
73 magmatic hydrothermal events ([Banks \*et al.\* 1994](#), [Salvi and Williams-Jones 2006](#)). These later  
74 processes may lead to their redistribution, fractionation and/or focused concentration.  
75 Geothermal brines were even considered as a potential source of the REEs for future industrial  
76 extraction ([Smith \*et al.\* 2017](#)).

77           Hydrothermal mobilization and transport of the REEs (as well as of other metals) from  
78 a parent magmatic body or metal-bearing rock is provided by water, preferentially in the form  
79 of aqueous complexes with the most abundant ligands in the crust. The knowledge about this  
80 complexation is a key for the understanding of the transporting capacities of hydrothermal  
81 fluids (*e.g.*, [Seward \*et al.\* 2014](#) and refs. therein). The first studies of the REEs solubilities in  
82 hydrothermal fluids implied their complexation with chloride, fluoride and sulfate anions (*e.g.*,  
83 [Banks \*et al.\* 1994](#), [Salvi and Williams-Jones 2006](#)), later acetate anions and hydrocarbons were  
84 found to be important for some specific geological environments (*e.g.*, [Lecumberri-Sanchez \*et\*](#)  
85 [al. 2018](#)); finally, there is growing evidence that carbonate ligands could be also involved into  
86 the hydrothermal mobilization of the REEs ([Fan \*et al.\* 2004](#), [Liu \*et al.\* 2018](#), [Vasyukova and](#)  
87 [Williams-Jones 2018](#)).

88           In our particular case, we study the role of carbonate and bicarbonate ligands in the  
89 hydrothermal transport of the REEs. During this research, we carried out autoclave experiments  
90 and faced the necessity of determining the trace quantities of the REEs in experimental  
91 products, including solutions with high mass fractions of sodium comparable with those in  
92 seawater (up to 3.0 % m/m). Another area of our study is focused on monazite interaction with  
93 hydrothermal brines with high concentrations of alkali and alkali earth metals originating from  
94 seawater evaporites. These two types of experiments have led us to seek the best method for  
95 the REEs quantification in solutions in terms of implementation time, cost of analyzes as well as

96 accuracy, precision and limits of detection. Here, we compare two different strategies that  
97 could be applied for the REEs quantification using ICP-MS: direct liquid microvolume analysis  
98 using the LA-ICP-MS versus the chromatographic separation of a sample matrix followed by  
99 pneumatic nebulization ICP-MS analysis.

100

## 101 **2. Overview of ICP-MS methods for REE quantifications in geological samples**

102

### 103 **2.1. ICP-MS for quantification of the rare earth elements in natural samples – alternatives, 104 advantages, and choice of mass-spectrometer configuration**

105

106 Since the development of inductively-coupled plasma-mass-spectrometry (ICP-MS) in  
107 the early 1980s ([Houk \*et al.\* 1980](#); [Date and Gray 1981, 1983](#)), this method is widely used to  
108 determine the REEs in natural samples. As an alternative to the MS, the trace quantities of REE  
109 could be also measured using inductively coupled plasma-atomic emission spectroscopy (ICP-  
110 AES), instrumental neutron activation analysis (INAA) and high-performance ion  
111 chromatography (HPIC). Another way of sample ionization, except for ICP that is commonly  
112 used for the REEs analyses, is thermal ionization, in particular, isotope dilution-thermal  
113 ionization mass spectrometry (ID-TIMS). Details about the advantages and negative aspects of  
114 the listed techniques could be found elsewhere (*e.g.*, [Ishikawa \*et al.\* 2003](#)). Briefly, ICP-MS is a  
115 method of choice for the REEs quantification if: i) a precise quantification of all the REEs  
116 including the monoisotopic (Pr, Tb, Ho, and Tm) is needed, ii) the REEs mass fractions in samples  
117 are expected to be at the level of 1  $\mu\text{g g}^{-1}$  and below, iii) samples are unique and limited  
118 quantities of material are available for analyses, and iv) the nuclear reactor facilities are not

119 accessible: nowadays INAA is practically replaced by ICP-MS due to its complexity and  
120 associated costs.

121 In our case, we used a single collector quadrupole based ICP-MS unit either coupled  
122 with a laser ablation unit, or equipped with traditional nebulization and spray chamber, in order  
123 to compare the results of the REEs measurements with the two different ways of sample  
124 solution introduction into ICP. Here, we compare the direct laser ablation of experimental  
125 solutions loaded into glass capillaries and the classical injection of experimental solutions  
126 aerosols after their matrix isolation using column chromatography with strong cation-exchange.  
127 Alternative ICP-MS systems, such as sector-field (sf-ICP-MS) or time of flight (TOF) systems that  
128 both can have either single or multiple collector detection system (e.g., [Sindern 2017](#)) are out of  
129 the scope of the present study.

130 By using single collector quadrupole ICP-MS we assume, that the ratio of stable isotope  
131 of the REEs in our samples have a chondritic isotope composition, thus, only one isotope of  
132 each REE can be acquired to obtain the element concentration in a sample. However, we  
133 measured a few isotopes of the same REE (where available) during ICP-MS analysis to verify any  
134 biases due to uncorrected interferences.

135

## 136 **2.2. Sample preparation of rocks, minerals and natural fluids applied for ICP-MS analyses** 137 **of the Rare Earth Elements**

138

139 During previous studies of the REEs quantification by ICP-MS, two main analytical  
140 issues were identified: 1) low abundances of the REEs in some natural objects that approach the  
141 detection limits of ICP-MS method (e.g., sub ng g<sup>-1</sup> level in residual ultramafic rocks; [Nakamura](#)  
142 [and Chang 2007](#); [Ulrich et al., 2012](#)), and 2) a strong matrix effect. High concentrations of matrix

143 elements in solutions (essentially Si, F and NaCl-rich solutions obtained from digested quartz  
144 after crush-leach procedures) induce an enhancement or a suppression of the analytical signal,  
145 ([Ghazy et al. 1993](#)). For example, [Eaton et al. \(1992\)](#) detected a progressive signal suppression  
146 as the salt (NaCl) concentration in the sample solution was increased. These findings  
147 determined the main sample preparation procedures for the REEs analysis by ICP-MS: matrix  
148 elimination and target elements preconcentration followed by an introduction of sample  
149 solution into ICP.

150           The ion exchange resins are commonly used in chromatography and ICP-MS analysis  
151 for element separations. Conventional ion exchange resins consist of a cross-linked polymer  
152 matrix with a relatively uniform distribution of ion-active sites. A cross-link is a bond that links  
153 one polymer chain to another. The degree of cross-linking (DC), expressed quantitatively as the  
154 mole percent, relates to the number of groups that interconnect the polymerization mixture.  
155 The DC affects the kinetics of the cation-exchange process ([Michaud 2011](#), [Kołodziejka et al.](#)  
156 [2019](#)). The resin AG 50W<sup>®</sup> is commonly used for REEs isolation from the matrix. It is composed  
157 of sulfonic acid functional groups attached to a styrene-divinylbenzene (S/DVB) copolymer  
158 lattice: the strands of polystyrene (S) are held together by DVB and X8 or X12 means DC = 8% or  
159 DC = 12%, respectively (here, the mole percent of DVB in the (S/DVB) copolymer lattice). [Luais](#)  
160 [et al. \(1997\)](#) used a column of strong cation-exchange resin AG 50W<sup>®</sup>X12 in HCl acid media for  
161 high-precision isotope ratios measurements of neodymium and samarium in basalt samples  
162 (Reunion Island, Indian Ocean) using a multiple collector ICP-MS (MC-ICP-MS). This method  
163 allowed to isolate Heavy Rare Earth Elements and Yttrium (HREEs+Y) from the light and medium  
164 REEs (LREEs+MREEs). In the subsequent studies the REEs separation protocol mentioned above  
165 was combined with the other procedures of element separation to study the behavior of  
166 multiple isotopic systems during fluid-related deformation zone of leucogranite from the French

167 Massif Central (Luais *et al.* 2009) and metamorphic dehydration–hydration in eclogite and  
168 amphibolite samples from the Western Gneiss Region in Norway (Martin *et al.* 2010).

169 Cation exchange resins methods before REE+Y measurements using ICP-MS techniques is  
170 required in some specific cases for precisely and accurately determine REE+Y contents, such as  
171 accurate measurements of geological reference materials (JGb2 leucogabbro and JR3  
172 peralkaline rhyolite from the Geological Survey of Japan) (Lee *et al.* 2000). This also ensures a  
173 pre-concentration of REE in highly depleted lithologies, such as ultra-depleted in REEs  
174 peridotites (Ulrich *et al.* 2012). or REE separation from highly charged matrix such as salts  
175 (Steinman *et al.* 2001). Halicz *et al.* (1996) similarly, developed an on-line preconcentration  
176 method for ICP-MS to quantify the REEs in seawaters and highly saline brines.

177 Here, on the basis of previous analytical developments acquired for solid samples in  
178 CRPG (Nancy, France) and ISTERre (Grenoble, France) laboratories, we customize an offline  
179 isolation protocol for brines, with highly-charged matrix, typical to our experimental systems.

180

### 181 **2.3. LA-ICP-MS as a tool for express quantification of the REEs in solutions**

182

183 LA-ICP-MS analyses of the REEs in minerals and fluid inclusions have already been  
184 performed successfully to tackle scientific issues such as abundance and fractionation of the  
185 REEs in natural minerals and fluid inclusions (Leisen 2011), genesis of uranium deposits  
186 (Mercadier *et al.* 2011, Lach *et al.* 2013), geochronometric dating of rocks and minerals using  
187 the radioactive REE isotopes  $^{138}\text{La}$ ,  $^{147}\text{Sm}$  and  $^{176}\text{Lu}$  (Sindern 2017), mineralogy of the REEs in  
188 coal fly ash (Thompson *et al.* 2018), partial resettling of the U-Th-Pb geochronometers during  
189 monazite recrystallization (Grand'Homme *et al.* 2018), adsorption of the REEs on aluminum and

190 iron (oxy)-hydroxides in bauxites (Mondillo *et al.* 2019) and variety of fluids origin in iron oxide-  
191 copper-gold ore deposits revealed by the REEs signatures in fluorites (Schlegel *et al.* 2020).

192 LA-ICP-MS is widely used in geosciences due to the unique combination of its spatial  
193 resolution, fast acquisition of results and low detection limits which are supported by  
194 reasonable analytical costs. Spatial resolution is critical for some minerals and fluid inclusion  
195 assemblages that have micrometer to millimeter scale, overgrowths and zoning of minerals  
196 related to successive geological events. Thus, a spatially resolved analysis at an appropriate  
197 scale is the only way to determine the evolution of the mineral composition through time and  
198 thereby decipher multiple processes related to geochemical evolution during single crystal  
199 growth (*e.g.*, Lach *et al.* 2013).

200 The use of LA-ICP-MS for solutions historically originates from the challenging studies  
201 of mineral fluid inclusions, that are complicated by very small quantities of solution in individual  
202 fluid inclusions typically ranging from  $10^{-13}$  to  $10^{-6}$  g (Roedder 1984). However, it was shown  
203 that this method could be also used for a small quantity of any aqueous solution (*e.g.*, standard  
204 or experimental) loaded into pure silica capillary that could be then ablated by laser like a fluid  
205 inclusion (Leisen *et al.* 2012a,b, Harlaux *et al.* 2015, Grand'Homme *et al.* 2018). The matrix  
206 effects for elemental analyses using LA-ICP-MS were widely discussed in literature (*e.g.*,  
207 Günther *et al.* 1998, Velásquez *et al.* 2012, Leisen *et al.* 2012a, Grand'Homme *et al.* 2018).  
208 Liquid samples can be quantitatively analyzed by their introduction into glass capillaries without  
209 any additional chemical treatment using NIST SRM glasses as reference materials and precisely  
210 quantified sodium concentrations as an internal standard (Günther *et al.* 1998). This procedure,  
211 which uses solid reference materials to quantify the REEs mass fractions in aqueous solution, is  
212 carefully validated in this study.

213

## 214 3. Experimental

215

### 216 3.1. Experimental conditions and setup of hydrothermal reactors

217

218 The solubilities of the REEs were studied in the following carbon-bearing and carbon-  
219 free systems at 100, 150, 200, and 250°C and at pressures ranging from 20 to 150 bar (Table 1).

220 Hydrothermal reactors were developed to combine injection and sampling of solutions in a  
221 multi-phasic system at high temperatures and pressures with the monitoring of pH in-situ. The

222 detailed description of the experimental setup could be found elsewhere (e.g., Truche *et al.*

223 2016). Briefly, we used commercial bolt-closure reactors (Parr Instrument©) made of pure

224 titanium (grade 3). The body and the head of the reactors were sealed with a PTFE gasket. The

225 maximum working temperature and pressure of the reactors were 300°C and 200 bar,

226 respectively. The internal volumes of the vessels varied from 250 to 500 ml. The temperature

227 was monitored using an immersed thermocouple and was held constant within  $\pm 1^\circ\text{C}$  by an

228 electric furnace. The vessel was equipped with several connections that enabled regular

229 sampling and injection of fluids, as well as adjustment of the working pressure.

230

231 **Table 1.** Summary of the experiments with the REE oxides conducted in this study.

232

233 The reactors were filled to two-thirds of their volume with an experimental solution.

234 The solution and the pressure vessel were bubbled and flushed with argon for half an hour to

235 remove dissolved nitrogen and oxygen. After flushing with argon, the autoclaves were leak

236 checked at ambient temperature at a pressure of 60 bar. The experimental solutions and solids

237 were stirred at 200 rpm by an impeller driven by an external magnetic driver. Aliquots of

238 solution (2-3 g) were regularly sampled during the experiments. The first sample during one  
239 sampling session served to remove the dead volume from the sampling tubes and to measure  
240 the pH at ambient conditions. The second sample was filtered through a 0.2  $\mu\text{m}$  PTFE filter and  
241 acidified with 2 wt. %  $\text{HNO}_3$  solution (dilution factor 10) for the subsequent ICP-OES analyses of  
242 sodium and determination of the REEs using LA-ICP-MS and ICP-MS.

243

### 244 **3.2. Chemical reagents used for the hydrothermal experiments**

245

246 The initial solid phases of the REEs used for the hydrothermal experiments were the  
247 following oxide powders: yttrium oxide  $\text{Y}_2\text{O}_3$  (Rare Earth Products Ltd., 99.999 % m/m, CAS №  
248 1314-36-9), lanthanum oxide  $\text{La}_2\text{O}_3$  (Sigma-Aldrich, 99.99 % m/m, CAS № 1312-81-8), cerium  
249 oxide  $\text{CeO}_2$  (Prolabo Rhône-Poulenc Ltd., 99.9 % m/m, CAS № 1306-38-3), praseodymium oxide  
250  $\text{Pr}_2\text{O}_3$  (Rhône-Poulenc Industries, 99.99%, CAS № 12036-32-7), neodymium oxide  $\text{Nd}_2\text{O}_3$  (Sigma-  
251 Aldrich, 99.9 % m/m, CAS № 1313-97-9), samarium oxide  $\text{Sm}_2\text{O}_3$  (Sigma-Aldrich, 99.9 % m/m,  
252 CAS № 12060-58-1), europium oxide  $\text{Eu}_2\text{O}_3$  (Rhône-Poulenc Industries, 99.99 % m/m, CAS №  
253 1308-96-9), gadolinium oxide  $\text{Gd}_2\text{O}_3$  (Sigma-Aldrich, 99.9 % m/m, CAS № 12064-62-9),  
254 dysprosium oxide  $\text{Dy}_2\text{O}_3$  (Sigma-Aldrich, 99.99 % m/m, CAS № 1308-87-8), erbium oxide  $\text{Er}_2\text{O}_3$   
255 (Sigma-Aldrich, 99.99 % m/m, CAS № 12061-16-4), ytterbium oxide  $\text{Yb}_2\text{O}_3$  (Sigma-Aldrich, 99.99  
256 % m/m, CAS № 1314-37-0). The mass of each oxide powder loaded into the autoclave was  $\sim 100$   
257 mg in all the experiments. Experimental solutions were prepared using the following salts:  
258  $\text{Na}_2\text{CO}_3$  (Roth,  $\geq 99.5$  % m/m, ACS, anhydrous, CAS № 497-19-8) and  $\text{NaHCO}_3$  (Sigma Aldrich,  
259  $\geq 99.7$  % m/m, ACS, anhydrous, CAS № 144-55-8). An aqueous solution of  $\text{HNO}_3$  (2 % m/m) was  
260 prepared from a bi-distilled acid.

261

262 **3.3. Certified reference materials (CRM) used for ICP-MS, LA-ICP-MS and ICP-OES analyses**  
263 **and standard solutions preparation**

264  
265 All chemical procedures were carried out in clean room conditions. Preparation of  
266 reactants, standard solutions, and dilutions were performed by weight and using high purity  
267 18.2 MΩ cm MQ water (Elga Chorus system®) was used through this study. HCl and HNO<sub>3</sub> acids  
268 were purified by double distillation using a Savillex™ DST-1000 sub-boiling distillation system  
269 (Savillex, USA).

270 Calibration curves for the REEs analyses by ICP-MS were established relative to  
271 standard solutions containing 1, 10, 25 and 50 ng g<sup>-1</sup> of the REEs in HNO<sub>3</sub> matrix (2 % m/m).  
272 These standard solutions were prepared by weighting the certified CRM standard solution REE  
273 mix TraceCERT® Co. LLC Sigma-Aldrich, 16 elements, 50 mg l<sup>-1</sup> in 2 % m/m nitric acid. Standard  
274 solutions containing 100 and 500 ng g<sup>-1</sup> of the REEs were also prepared and analyzed as  
275 additional standards to check the linearity of the obtained calibration curves, which was useful  
276 for analyses of the most concentrated samples.

277 Standard solutions with high contents of matrix elements (sodium, potassium,  
278 magnesium and calcium) were prepared to establish the off-line quantification protocol for the  
279 REEs separation from a charged matrix using cation-exchange resin. The following salts were  
280 weighted with the REE mix and yttrium CRM solutions and Milli-Q water: MgCl<sub>2</sub>·6H<sub>2</sub>O (Prolabo),  
281 CaCl<sub>2</sub>·2H<sub>2</sub>O (Merck), NaCl (99.5 % m/m, Acros Organics), KCl (99.5 % m/m, Roth pa ACS ISO  
282 Reagent). The prepared standard solutions were analyzed for major cations in SARM (CRPG,  
283 Nancy) using ICP-OES Thermo Fischer ICap 6500. An analytical signal calibration of sodium  
284 during ICP-OES analyses was performed using the sodium CRM for ICP (TraceCERT® Co. LLC  
285 Sigma-Aldrich, 1000 mg l<sup>-1</sup> Na in 2 % m/m nitric acid).

286 Standard solutions containing 10 ng g<sup>-1</sup>, 100 ng g<sup>-1</sup>, 1 µg g<sup>-1</sup> and 10 µg g<sup>-1</sup> of the REEs  
287 in the matrix of aqueous NaCl solution (1 mol l<sup>-1</sup>) were prepared to test the accuracy of LA-ICP-  
288 MS analyses. These standard solutions were prepared from the diluted REEs CRM (TraceCERT®  
289 16 elements mentioned above) and NaCl salt (99.5 % m/m, Acros Organics). Sodium was added  
290 into the standard solutions to be used as an internal standard for all LA-ICP-MS analyses.  
291 Sodium concentrations in standard solutions and in experimental samples were measured by  
292 ICP-OES in SARM (CRPG, Nancy). The standard solutions with known amount of Na were loaded  
293 into glass capillaries.

294 The CRM glasses NIST SRM 610 and NIST SRM 612 (matrix composition SiO<sub>2</sub> 72 % m/m,  
295 Na<sub>2</sub>O 14 % m/m, CaO 12 % m/m, Al<sub>2</sub>O<sub>3</sub> 2 % m/m) were used as calibrators for LA-ICP-MS. These  
296 glasses are certified for a limited number of elements by NIST. Thus, following ISO guidelines  
297 and the protocol of the International Association of Geoanalysts, the reference values for the  
298 REEs in NIST SRM 610 and NIST SRM 612 were taken from [Jochum \*et al.\* \(2011\)](#).

299

#### 300 **3.4. Chromatographic isolation and ICP-MS analyses of the REEs in experimental solutions**

301

302 Polypropylen columns (Triskem® 10 cm high and 1.5 cm internal diameter) were filled  
303 with AG 50W® cation-exchange resin (200-400 mesh, hydrogen form) with a degree of cross-  
304 linking of 8 mol % (or 12 mol % for some calibration tests). Considering the large amount of  
305 matrix with respect to the REEs contents (~60 g l<sup>-1</sup> of chloride salts vs ~60 mg l<sup>-1</sup> of the REEs for  
306 the calibration tests), a resin volume of 20 ml was used in order to avoid resin saturation. The  
307 matrix-rich REE standard solutions and sampled experimental solutions were slowly evaporated  
308 to dryness at 90°C in Savillex® PTFE vials. The residue was dissolved in 5 ml of HCl (2.0 mol l<sup>-1</sup>)  
309 and loaded onto resin pre-cleaned with alternately HCl (6 mol l<sup>-1</sup>) and MQ water and

310 conditioned by 20 ml of HCl (2 mol l<sup>-1</sup>). After complete elution of sodium (or complete elution  
311 of Na, Mg, K, and ~75 % m/m of Ca for the case of calibration tests) with 90 ml HCl solution (2.0  
312 mol l<sup>-1</sup>), the fraction containing the REEs was collected in Savilex® Teflon vials with 155 ml of  
313 HCl solution (6.0 mol l<sup>-1</sup>). The REEs fraction was evaporated to dryness at 90°C and redissolved  
314 in 10 ml HNO<sub>3</sub> 2 % m/m solution for the subsequent ICP-MS analyses. All chromatographic  
315 isolation and evaporation steps were made in cleanroom conditions.

316 The REEs mass fractions in solutions were measured using the quadrupole ICP-MS X-  
317 Series 2 ThermoScientific at CRPG laboratory (Nancy, France) (Table 2). The selected isotopes  
318 for REE quantification, and corresponding instrumental detection and quantification limits  
319 obtained after ten parallel measurements of matrix solution HNO<sub>3</sub> (2 % m/m) are reported in  
320 Table 3. Detection limits for all the REEs were determined as the mass fraction equivalent of  
321 three times the standard deviation of the procedural blank. They range from 0.1 pg g<sup>-1</sup> for Lu to  
322 5 pg g<sup>-1</sup> for La and 20 pg g<sup>-1</sup> for Y, and are better than published values published, e.g., from 1  
323 to 120 pg g<sup>-1</sup> (Ulrich et al. 2012). Our detection limits are significantly lower relative to the REE  
324 mass fractions of all the experimental solutions analyzed in this work and are systematically  
325 lower than the REE contents determined in procedural blanks after the use of the chemical  
326 protocol that is described below (Table 6).

327

328 **Table 2.** Instrumental operating parameters for ICP-MS.

329

330 **Table 3.** The detection limits (DL, 3σ) and the quantification limits (QL, 10σ) for the ICP-MS  
331 analyses of the REEs, reported in pg g<sup>-1</sup>.

332

333 **3.5. LA-ICP-MS analyses of experimental solutions**

334  
335 LA-ICP-MS analyses of experimental solutions were carried out at the GeoRessources  
336 laboratory (Nancy, France). The LA-ICP-MS setup is composed of a 193 nm GeoLas Excimer laser  
337 (ArF, Microlas, Göttingen, Germany), with a microscope for sample observation and laser beam  
338 focus onto the sample, and an Agilent 7500c quadrupole ICP-MS. The experimental solutions  
339 were loaded into pure silica capillaries (320  $\mu\text{m}$  int  $\varnothing$ , 435  $\mu\text{m}$  ext  $\varnothing$ , <sup>®</sup>Polymicro-Technologies).  
340 For each experiment, the lanthanides, <sup>89</sup>Y, and <sup>23</sup>Na were analyzed. Data were collected with an  
341 integration time of 0.01 s per channel for <sup>23</sup>Na, <sup>28</sup>Si, <sup>29</sup>Si, 0.02 s for <sup>89</sup>Y, <sup>139</sup>La, <sup>140</sup>Ce, <sup>141</sup>Pr, <sup>146</sup>Nd,  
342 <sup>147</sup>Sm, <sup>153</sup>Eu, 0.03 s for <sup>157</sup>Gd, <sup>159</sup>Tb, <sup>163</sup>Dy, <sup>165</sup>Ho, <sup>166</sup>Er, <sup>169</sup>Tm, <sup>172</sup>Yb, and <sup>175</sup>Lu. Data were  
343 acquired as raw counts per second (cps) using the time-resolved mode. For each analysis  
344 (reference material and sample), the background was measured for 30 s, and the overall signal  
345 acquisition was recorded for 100 s. The glass reference materials NIST SRM 610 and NIST SRM  
346 612 (Jochum et al. 2011) were used as reference materials, whereas sodium concentrations in  
347 solutions preliminary quantified using ICP-OES were used as an internal standard (for details see  
348 section 2.3). The spot size of 60  $\mu\text{m}$  was used. The data reduction (quantification and limits of  
349 detection) was carried out using Iolite software (Paton et al. 2011) based on the equations  
350 developed by Longerich et al. (1996). More details on instrumental operating parameters are  
351 reported in Table 4.

352

353 **Table 4.** Instrumental operating parameters for LA-ICP-MS.

354

355

356

357

## 358 4. Results

359

### 360 4.1. Calibration tests and choice of the cation-exchange resin, validation of analytical 361 protocol of off-line sample preparation for ICP-MS analysis of the REEs

362

363 Seven tests of column calibration on standard solutions were performed during this  
364 study. The off-line protocol for the REEs separation from sodium-rich matrix, *e.g.*, type of resin,  
365 concentrations and volumes of acids, was established from calibration tests with simulated Na-  
366 K-Mg-Ca-rich standard solutions (Table 3). Using these solutions, we selected the type of cation-  
367 exchange resin, as well as molarities and volumes of HCl acids used for subsequent elution of  
368 matrix and the REEs. The cation exchange columns were calibrated to obtain the best yields  
369 ( $100\pm 7\%$ ) for the REEs using minimal volumes of acids during the elution process (Fig. 1). The  
370 two AG 50W<sup>®</sup> resins (200-400 mesh) with 8 and 12 mol % cross-linkage were tested for this  
371 purpose. The AG50W-X8 resin (8 mol % in DVB) was chosen because the use of AG50W-X12 (12  
372 mol % in DVB) required more than 225 mL of HCl 6.0 mol l<sup>-1</sup> solution to quantitatively collect all  
373 the REEs from the column, rising issues concerning procedural blanks, sample throughput and  
374 reactive consumption.

375 Here we report only the result of the last calibration with complete isolation of the  
376 REEs. A volume of 5 ml of the standard solution in HCl (2.0 mol l<sup>-1</sup>), containing MgCl<sub>2</sub> 5.18 g l<sup>-1</sup>,  
377 CaCl<sub>2</sub> 10.01 g l<sup>-1</sup>, NaCl 15.93 g l<sup>-1</sup>, KCl 25.38 g l<sup>-1</sup>, lanthanides and Sc 3.85 mg l<sup>-1</sup>, and Y 8.27 mg  
378 l<sup>-1</sup>, was loaded into the column. This matrix composition was chosen to simulate a composition  
379 of typical natural brine that always contains high concentrations of the alkaline and alkaline  
380 earth elements (see chapter 1.1 for details). Sodium, magnesium, and potassium were  
381 completely removed from the resin after the elution with 90 ml of HCl solution (2.0 mol l<sup>-1</sup>),

382 whereas calcium was removed incompletely (76%) (Table 5, Fig. 1c). In our experimental study  
383 with carbonates, only sodium needed to be carefully isolated from the REEs, because its  
384 preferential ionization compared with other elements can disturb their ionization, thus, so we  
385 have not further refined the presented extraction protocol. The elution of the REEs with HCl  
386 solution (6.0 mol l<sup>-1</sup>, 155 cm<sup>3</sup>) was complete during the final calibration, in the order HREEs  
387 (~40 ml), MREEs (~25 ml), and finally LREEs (~90 ml), with the REEs yields in the uncertainty  
388 range of 100±7% (Table 3). A complete Ca extraction of calcium could be reached by an  
389 increasing the HCl 2.0 mol l<sup>-1</sup> volume of matrix elution, but not by increasing HCl molarity to 2.5  
390 mol l<sup>-1</sup> that would induce early elution of HREEs in the matrix fraction.

391  
392 **Fig. 1.** a) Photo of cation exchange resin; a) schematic illustration of a cation-exchange process  
393 in a column; a) elution of Na, Mg, K, Ca matrix with HCl 2.0 mol l<sup>-1</sup> solution; b) subsequent  
394 removal of the REEs during elution with HCl 6.0 mol l<sup>-1</sup>.

395  
396 **Table 5.** Results of the final calibration of cation-exchange resin column AG 50W<sup>®</sup>X8 (200-400  
397 mesh).

398  
399 Blank solutions of high purity 18.2 MΩ cm water and aqueous solutions of NaCl (1 mol  
400 l<sup>-1</sup>) were treated like experimental samples to quantify the procedural blanks. The obtained  
401 mass fractions of the REEs in the blank solutions varied from 2 to 650 pg g<sup>-1</sup> (Table 6)  
402 depending on the REE and could not affect the outcome of our analytical results that are at the  
403 10 ng g<sup>-1</sup> level, with the exception of the lowest mass fractions of Ce, La, and Nd analyzed  
404 during this study. The obtained mass fractions of these elements were corrected for procedural  
405 blank levels.

406

407 **Table 6.** The REEs mass fractions in blank and standard solutions after the use of a cation  
408 exchange resin column, reported in  $\mu\text{g g}^{-1}$ .

409

410 The analytical protocol for REEs separation from sodium for the subsequent ICP-MS  
411 analyses established during this study includes the following procedures:

- 412 i) weighing of the sample solutions;
- 413 ii) evaporation of solutions to dryness at  $90^{\circ}\text{C}$  and residue dissolution in 5 ml of HCl  
414  $2.0 \text{ mol l}^{-1}$ ;
- 415 iii) preparation of the cation exchange resin columns filled with  $10 \text{ cm}^3$  volume resin  
416 (AG<sup>®</sup> 50W-X8 200-400 mesh);
- 417 iv) conditioning of the resin with HCl  $2.0 \text{ mol l}^{-1}$  (20 ml)
- 418 v) loading of the prepared samples
- 419 vi) add 90 ml of HCl  $2.0 \text{ mol l}^{-1}$  in each column for matrix elution
- 420 vii) add 155 ml of HCl  $6.0 \text{ mol l}^{-1}$ , for complete REE elution, and collection into Teflon  
421 vials .
- 422 viii) evaporation of the HCl  $6.0 \text{ N}$  REE-bearing fraction to dryness, at  $90^{\circ}\text{C}$  on a hot  
423 plate.
- 424 ix) redissolution of the dry residue in 10 ml of  $\text{HNO}_3$  2 % m/m (ultrasonic bath);
- 425 x) weighing of the obtained  $\text{HNO}_3$  solutions and calculation of dilution factors.

426

427 In order to estimate the accuracy of our off-line analytical protocol for the REEs  
428 separation from saline matrix described above, REE-bearing standard solutions doped with high  
429 contents of sodium, potassium, magnesium, and calcium (Table 6) were treated in the same  
430 manner as our experimental samples. The measured concentrations of the REEs are in a  
431 reasonable agreement with the REEs concentrations of prepared standard solutions, with an  
432 accuracy estimated within  $\pm 10\%$  (3 SD) for the mass fraction range between 25 and  $100 \text{ ng g}^{-1}$ .  
433 This is similar to the calibration test performed for standard solution ( $\pm 7\%$ ) (Table 5) for  $\sim 1$  to

434 ~10  $\mu\text{g g}^{-1}$  REEs mass fractions. Our analytical protocol is validated for the lanthanides and  
435 yttrium measurements with a  $\pm 10\%$  accuracy, within a mass fraction range from ~10  $\text{ng g}^{-1}$  to  
436 ~10  $\mu\text{g g}^{-1}$ . The reported accuracy estimation is comparable with the repeatability of the ICP-  
437 MS analysis for the same solution, whereas RSD for an individual analysis typically varied  
438 between 3 and 5%.

439

#### 440 **4.2. Accuracy and repeatability of LA-ICP-MS analyses of the REEs in solutions with** 441 **simulated matrix loaded in glass capillaries, reproducibility of NIST SRM glasses** 442 **analyses**

443

444 The accuracy of LA-ICP-MS analyses was verified by using standard solutions prepared  
445 by weighing (see section 2.3). Typical time resolved LA-ICP-MS signals and the REEs responses  
446 during capillary ablation are shown in [Fig. 2](#). Limits of detection for each REE, as well as chosen  
447 isotopes, are reported in [Table 7](#). Typical relative standard deviations (RSD, %) for an analytical  
448 signal obtained on standard solutions during LA-ICP-MS measurements were found to be below  
449 20% for the mass fraction range from 100  $\text{ng g}^{-1}$  to 10  $\mu\text{g g}^{-1}$  for all the REEs and about 50-60%  
450 for a standard solution containing 10  $\text{ng g}^{-1}$  of the REEs. Accuracy and repeatability between  
451 measurements obtained by multiple ablations of the same standard solutions are illustrated in  
452 [Fig. 3](#) and are reported in the [Electronic Supplementary Material](#). Analyses of standard solutions  
453 with the REEs mass fractions lower than 1  $\mu\text{g g}^{-1}$  are less accurate, with deviation from the  
454 regression line towards lower measured values.

455

456 **Table 7.** Mean values of detection (DL) and quantification (QL) limits acquired on standard  
457 solutions during one analytical LA-ICP-MS session, in ng g<sup>-1</sup>. Note that for individual analyses,  
458 the best DL values could reach ~10 ng g<sup>-1</sup>.

459

460 **Fig. 2.** LA-ICP-MS analyses of the REEs in standard solutions.

461

462 **Fig. 3.** Results of the REEs analyses in standard solutions obtained using LA-ICP-MS (results for  
463 other REEs are available in the Electronic Supplementary Material). Note the deviation to lower  
464 values for some standard solutions with REE mass fractions lower than 1 µg g<sup>-1</sup>.

465

466 The both reference materials - NIST SRM 610 and NIST SRM 612 - were measured twice  
467 before and after each analytical session. The NIST SRM 612 glass was quantified for the REEs as a  
468 sample: certified sodium concentration in NIST SRM 612 glass served as an internal standard and  
469 NIST SRM 610 glass served as a calibrator. The average error between the two quantifications of  
470 the REEs in NIST SRM 610 and NIST SRM 612 reference materials vary from 0,1 to 7% for all the  
471 REEs in both glasses ([Electronic Supplementary Material](#)).

472

## 473 **5. Discussion**

474

### 475 **5.1. Comparison of the REEs quantification in experimental solutions with two** 476 **introduction systems for quadrupole ICP-MS measurements: laser ablation and** 477 **pneumatic nebulization after matrix purification**

478

479 The mass fractions of rare earth elements (including Y) in the experimental solutions

480 obtained using direct LA-ICP-MS and ICP-MS with pneumatic nebulizer (hereafter, pn-ICP-MS)  
481 after matrix isolation are reported in [Tables 8-11](#) and graphically presented in [Fig. 4](#).

482 As a whole, the mass fractions of the REEs measured in acidified experimental solutions  
483 ([Fig. 4](#)) are in a very good agreement with pn-ICP-MS for the case of Ce, Pr, Eu, Er and Yb within  
484 associated analytical uncertainties (~18-22%). Yttrium, Nd, Sm and Dy were well quantified  
485 within their typical RSD and reproducibility values (~25-30%, [Tables 8-11](#)), whereas the data  
486 obtained for La and Gd are much less accurate (~47 and ~41% of the pn-ICP-MS values,  
487 respectively).

488 There are however few outliers for Ce. Indeed, few low Ce-samples (10-70 ng g<sup>-1</sup>)  
489 show LA-ICP-MS mass fractions systematically lower than those obtained by pn-ICP-MS, with,  
490 however, similar typical analytical uncertainties in terms of 3RSD (%) for both methods ([Tables](#)  
491 [8-11](#)). Such deviation towards low Ce mass fractions is also seen for LA-ICP-MS Ce analyses of  
492 standard solutions of same concentration range ([Fig. 3](#)). Then, it is improbable that for the low  
493 concentrations, cerium mass fractions are overestimated by pn-ICP-MS analyses after matrix  
494 separation of sample solutions and blank correction. The calculated Ce mass fractions of those  
495 samples by LA-ICP-MS, using the regression line equation in [Fig. 4](#), would be in the range of (12-  
496 85 ng g<sup>-1</sup>). Then, the observed discrepancy is more likely due to Ce concentrations being close  
497 to the detection limit of the LA-ICP-MS.

498  
499 **Table 8.** Fluid compositions of experimental samples in the H<sub>2</sub>O–NaHCO<sub>3</sub>–REEs system. LA-ICP-  
500 MS data. Uncertainty (measurement repeatability) is expressed in terms of 3RSD.

501  
502 **Table 9.** Fluid composition of experimental samples in the H<sub>2</sub>O–NaHCO<sub>3</sub>–REEs system. ICP-MS  
503 after ion-exchange resin Na-isolation. Uncertainty (measurement repeatability) is expressed in

504 terms of 3RSD.

505

506 **Table 10.** Fluid composition in the H<sub>2</sub>O–Na<sub>2</sub>CO<sub>3</sub>–REEs system. LA-ICP-MS data. Uncertainty  
507 (measurement repeatability) is expressed in terms of 3RSD.

508

509 **Table 11.** Fluid composition in the H<sub>2</sub>O–Na<sub>2</sub>CO<sub>3</sub>–REEs system. ICP-MS after ion-exchange resin  
510 Na-isolation. Uncertainty (measurement repeatability) is expressed in terms of 3RSD.

511

## 512 **5.2. Analyzing REEs in solutions by LA-ICP-MS**

513

514 The current practice of LA-ICP-MS analyses of the REEs in solutions using NIST SRM  
515 glasses as reference materials and sodium as an internal standard was further verified in the  
516 present study. Three types of matrix were ablated for the REEs analyses: synthetic silicate RM  
517 glasses NIST SRM 610 and NIST SRM 612, NaCl-rich neutral brines and NaNO<sub>3</sub>-rich acidified  
518 experimental solutions. The obtained results show that the presence of matrix effects for the  
519 REEs analyses in solutions could not be totally excluded for using NIST SRM glasses  
520 standardization, at least for the MS configurations with nanosecond laser. In NaCl-rich neutral  
521 brines all the REEs mass fractions analyzed with NIST SRM glasses are systematically  
522 underestimated by 4 to 40% compared to the REEs mass fractions in prepared standard  
523 solutions (Fig. 3). At the same time, for the case of acidified NaNO<sub>3</sub>-rich experimental samples  
524 the obtained results are systematically overestimated if we assume the data of nb-ICP-MS  
525 preceding by off-line sample preparation as real values (Fig. 4, Tables 8-11). Thus, the  
526 concentrations of the REEs in solutions could be both systematically overestimated and

527 underestimated by LA-ICP-MS depending on the nature of the sample (here, essentially  
528 presence of Si, Cl, N matrix elements and pH of analyzed solution).

529           The matrix effects on some REEs observed in this study sometimes exceed the  
530 analytical uncertainties reported both in terms of RSD (% ,  $3\sigma$  confidence level), reproducibility  
531 of multiple ablations of the same solution and cross-analysis of the two NIST SRM glasses using  
532 sodium as an internal standard. For example, the analyzed mass fractions of Er in NaCl-rich  
533 neutral brines are systematically underestimated by ~40% of the values known from the  
534 preparation procedure of the standard solutions (Fig. 3). Such a high discrepancy for Er exceeds  
535 both the estimated values of RSD (~30%,  $3\sigma$  confidence level) and reproducibility (~30%) from  
536 parallel LA-ICP-MS analyses, at least for the mass fractions above 100 ng g<sup>-1</sup>. However, for the  
537 same analytical session, the matrix effects for Nd, Sm and Gd are undistinguishable within the  
538 reported analytical uncertainties.

539           The solution matrix effects for the REEs vary in a very individual manner: the same REE  
540 could be well analyzed in one type of matrix using NIST SRM reference materials and be  
541 subjected to the matrix effect in another type of matrix as could be seen for Gd and Er (Table  
542 12). Thus, the NIST SRM calibration method works, but some systematic variations that were  
543 observed in the present study encourage us to recommend an additional calibration using the  
544 REEs standard solutions with adjusted matrix type, loaded in glass capillaries. The precision of  
545 analyses could be further improved by adding an isotope spike of a single element (*e.g.*, Sm or  
546 Nd) to sample solutions by weight and quantifying a single element with isotope dilution after  
547 LA-ICP-MS. Then this element can be used as precisely known internal standard to correct all  
548 other REEs for matrix effects.

549

550

551 **Fig. 4.** Comparison of the mass fractions of the REEs in solutions obtained using LA-ICP-MS and  
552 ICP-MS after sodium isolation.

553

## 554 **6. Conclusions**

555

556 The key points of this study are the following:

557 The established analytical protocol for the REEs quantification by ICP-MS in brines after  
558 matrix isolation with cation-exchange resin provides robust data for the REEs mass fractions as  
559 low as the 1 ng g<sup>-1</sup> level.

560 LA-ICP-MS analyses of solutions loaded into capillaries and classical pneumatic  
561 nebulization ICP-MS analyses after saline matrix isolation with cation exchange resin provide  
562 consistent results for the REEs quantification in brines in a range of mass fractions between 10  
563 ng g<sup>-1</sup> and 10 µg g<sup>-1</sup> within reported analytical uncertainties (RSD from 15 to 30% of a value for  
564 LA-ICP-MS). The precision level acquired during this study by LA-ICP-MS technique is acceptable  
565 and sufficient enough for the purposes of the experimental hydrothermal geochemistry.

566 LA-ICP-MS, being an express method, could be highly recommended for the REEs  
567 quantification in brines: in a single day of LA-ICP-MS analyses it is possible to measure up to 100  
568 capillaries with REE solution, while it takes one month of cleanroom REE isolations to produce  
569 these analyses with classical ICP-MS with pneumatic nebulizer. At the same time, the REEs  
570 isolation from the charged matrix with subsequent ICP-MS analysis provides more precise  
571 results ( $\pm 10\%$  a value within 3SD confidential level), and is required for the REEs mass fractions  
572 that are below the quantification limit of the LA-ICP-MS that was estimated at the  $\sim 100$  ng g<sup>-1</sup>  
573 level. These results provide a framework for the selection of analytical methods in future  
574 studies, depending on the required accuracy of REE quantification.

575  
576 **Acknowledgments**  
577  
578 This work was funded by the French National Research Agency through the "Investissements  
579 d'Avenir" National Research program (ANR-10-LABX-21–LABEX RESSOURCES21). M. Kokh  
580 acknowledges postdoctoral fellowship granted by Floralis UGA during the manuscript  
581 preparation. We thank D. Cividini (CRPG), D. Yeghicheyan (SARM, CRPG), S. Bureau (ISTerre) for  
582 their professional help with tedious sample preparations and ICP-OES chemical analyses. Special  
583 thanks go to Dr. Y. A. Kostitsyn (GEOKHI RAS) and Dr. S. M. Chernonozhkin (University Ghent)  
584 for the fascinating discussions of the trace elements quantification techniques in solutions,  
585 minerals and fluid inclusions. We are grateful to Dr. R. Mertz-Kraus for the handling of the  
586 manuscript and to the two anonymous reviewers that highly improved the quality of the  
587 present article.

## References

- 588
- 589
- 590 **Banks D.A., Yardley B.W.D., Campbell A.R. and Jarvis K.E. (1994)**
- 591 REE composition of an aqueous magmatic fluid: A fluid inclusion study from the Capitan Pluton, New
- 592 Mexico, U.S.A. **Chemical Geology**, **113**, 259-272, [https://doi.org/10.1016/0009-2541\(94\)90070-1](https://doi.org/10.1016/0009-2541(94)90070-1).
- 593
- 594 **Bau M. (1991)**
- 595 Rare-earth element mobility during hydrothermal and metamorphic fluid-rock interaction and the
- 596 significance of the oxidation state of europium. **Chemical Geology**, **93**, 219-230,
- 597 [https://doi.org/10.1016/0009-2541\(91\)90115-8](https://doi.org/10.1016/0009-2541(91)90115-8).
- 598
- 599 **Boyet M. and Carlson R.W. (2005)**
- 600 <sup>142</sup>Nd evidence for early (>4.53 Ga) global differentiation of the silicate Earth. **Science**, **309**, 576-
- 601 581, <https://doi.org/10.1126/science.1113634>.
- 602
- 603 **Chavagnac V., Ali H.S., Jeandel C., Leleu T., Destrigneville C., Castillo A., Cotte L., Waeles M.,**
- 604 **Cathalot C., Laes-Huon A., Pelleter E., Nonnotte P., Sarradin P.-M. and Cannat M. (2018)**
- 605 Sulfate minerals control dissolved rare earth element flux and Nd isotope signature of buoyant
- 606 hydrothermal plume (EMSO-Azores, 37°N Mid-Atlantic Ridge). **Chemical Geology**, **499**, 111-125,
- 607 <https://doi.org/10.1016/j.chemgeo.2018.09.021>.
- 608
- 609 **Cole C.S., James R.H., Connelly D.P. and Hathorne E.C. (2014)**
- 610 Rare earth elements as indicators of hydrothermal processes within the East Scotia subduction zone
- 611 system. **Geochimica et Cosmochimica Acta**, **140**, 20-38,
- 612 <https://doi.org/10.1016/j.gca.2014.05.018>.
- 613
- 614 **Date A.R. and Gray A.L. (1981)**
- 615 Plasma source mass spectrometry using an inductively coupled plasma and a high resolution
- 616 quadrupole mass filter. **Analyst**, **106**, 1255-1267,

617 <https://doi.org/10.1039/AN9810601255>.

618

619 **Date A.R. and Gray A.L. (1983)**

620 Development progress in plasma source mass spectrometry. **Analyst**, **108**, 159-165,

621 <https://doi.org/10.1039/AN9830800159>.

622

623 **Doucelance R., Bellot N., Boyet M., Hammouda T., and Bosq C. (2014)**

624 What coupled cerium and neodymium isotopes tell us about the deep source of oceanic  
625 carbonatites. **Earth and Planetary Science Letters**, **407**, 175–186.

626 <https://doi.org/10.1016/j.epsl.2014.09.042>.

627

628 **Eaton A. N., Hutton R. C. and Holland J. G. (1992)**

629 Application of flow injection sample introduction to inductively coupled plasma-mass spectrometry for  
630 geological analysis. **Chemical Geology**, **95**, 63-71, [https://doi.org/10.1016/0009-2541\(92\)90043-5](https://doi.org/10.1016/0009-2541(92)90043-5).

631

632 **Fan H.-R., Xie Y.-H., Wang K.-Y., Tao K.-J. and Wilde S.A. (2004)**

633 REE daughter minerals trapped in fluid inclusions in the Giant Bayan Obo REE-Nb-Fe deposit, Inner  
634 Mongolia, China. **International Geology Review**, **46**, 638-645, [https://doi.org/10.2747/0020-  
635 6814.46.7.638](https://doi.org/10.2747/0020-6814.46.7.638).

636

637 **Ghazi A. M., Vanko D. A., Roedder E. and Seeley R. C. (1993)**

638 Determination of rare earth elements in fluid inclusions in inductively-coupled mass spectrometry  
639 (ICP-MS). **Geochimica et Cosmochimica Acta**, **57**, 4513-4516, [https://doi.org/10.1016/0016-  
640 7037\(93\)90500-V](https://doi.org/10.1016/0016-7037(93)90500-V).

641

642 **González-Álvarez I. and Kerrich R. (2010)**

643 REE and HFSE mobility due to protracted flow of basinal brines in the mesoproterozoic Belt-Purcell  
644 Supergroup, Laurentia. **Precambrian Research**, **177**, 291–307,

645 <https://doi.org/10.1016/j.precamres.2009.12.008>.

646

647 **Grand'Homme A., Janots E., Seydoux-Guillaume A.M., Guillaume D., Magnin V., Hövelmann J.,**  
648 **Hörschen C. and Boiron M.-C. (2018)**  
649 Mass transport and fractionation during monazite alteration by anisotropic replacement. **Chemical**  
650 **Geology, 484**, 51-68, <https://doi.org/10.1016/j.chemgeo.2017.10.008>.

651

652 **Gratz R. and Heinrich W. (1998)**  
653 Monazite-xenotime thermometry. III. Experimental calibration of the partitioning of gadolinium  
654 between monazite and xenotime. **European Journal of Mineralogy, 10**, 579-588,  
655 <https://doi.org/10.1127/ejm/10/3/0579>.

656

657 **Günther D., Audétat A., Frischknecht R. and Heinrich C. A. (1998)**  
658 Quantitative analysis of major, minor and trace elements in fluid inclusions using laser ablation-  
659 inductively coupled plasma mass spectrometry. **Journal of Analytical Atomic Spectrometry, 13**,  
660 263–270, <https://doi.org/10.1039/A707372K>.

661

662 **Halicz L., Gavrieli I. and Dorfman E. (1996)**  
663 On-line method for inductively coupled plasma mass spectrometric determination of Rare Earth  
664 Elements in highly saline brines. **Journal of Analytical Atomic Spectrometry, 11**, 811-814,  
665 <https://doi.org/10.1039/JA9961100811>.

666

667 **Harlaux M., Borovinskaya O., Frick D. A., Tabersky D., Gschwind S., Richard A., Günther D.**  
668 **and Mercadier J. (2015)**  
669 Capabilities of sequential and quasi-simultaneous LA-ICPMS for the multi-element analysis of small  
670 quantity of liquids (pl to nl): insights from fluid inclusion analysis. **Journal of Analytical Atomic**  
671 **Spectrometry, 30**, 1945–1969, <https://doi.org/10.1039/C5JA00111K>.

672

673 **Heinrich W., Anders G. and Franz G. (1997)**

674 Monazite-xenotime miscibility gap thermometry. 1. An empirical calibration. **Journal of**  
675 **Metamorphic Geology**, **15**, 3-16, <https://doi.org/10.1111/j.1525-1314.1997.t01-1-00052.x>.  
676

677 **Houk R.S., Fassel V.A., Flesch G.D., Svec H.J., Gray A.L. and Taylor C.E. (1980)**  
678 Inductively coupled plasma as an ion source for mass spectrometric determination of trace elements.  
679 **Analytical Chemistry**, **52**, 2283-2289, <https://doi.org/10.1021/ac50064a012>.  
680

681 **Ishikawa T., Sugimoto K. and Nagaishi K. (2003)**  
682 Determination of rare-earth elements in rock samples by an improved high-performance ion  
683 chromatography. **Geochemical Journal**, **37**, 671-680, <https://doi.org/10.2343/geochemj.37.671>  
684

685 **Jochum K. P., Weis U., Stoll B., Kuzmin D., Yang Q., Raczek I., Jacob D. E., Stracke A.,**  
686 **Birbaum K., Frick D. A., Günther D. and Enzweiler J. (2011)**  
687 Determination of Reference Values for NIST SRM 610-617 Glasses Following ISO Guidelines.  
688 **Geostandards and Geoanalytical Research**, **35**, 397–429, [https://doi.org/10.1111/j.1751-](https://doi.org/10.1111/j.1751-908X.2011.00120.x)  
689 [908X.2011.00120.x](https://doi.org/10.1111/j.1751-908X.2011.00120.x).  
690

691 **Kajiya T., Aihara M. and Hirata S. (2004)**  
692 Determination of rare earth elements in seawater by inductively coupled plasma mass spectrometry  
693 with on-line column pre-concentration using 8-quinolinole-immobilized fluorinated metal alkoxide  
694 glass. **Spectrochimica Acta Part B: Atomic Spectroscopy**, **59**, 543–550,  
695 <https://doi.org/10.1016/j.sab.2003.12.019>  
696

697 **Kołodzyńska D., Fila D., Gajda B., Gęga J. and Hubicki Z. (2019)**  
698 Rare Earth Elements—separation methods yesterday and today. In: Inamuddin A. M. and Asiri A.  
699 (eds.), **Applications of Ion Exchange Materials in the Environment**, Springer (Cham), pp. 161-  
700 185, [https://doi.org/10.1007/978-3-030-10430-6\\_8](https://doi.org/10.1007/978-3-030-10430-6_8).  
701

702 **Lach P., Mercadier J., Dubessy J., Boiron M.-C. and Cuney M. (2013)**

703 In situ quantitative measurement of Rare Earth Elements in uranium oxides by Laser Ablation-  
704 Inductively Coupled Plasma-Mass Spectrometry. **Geostandards and Geoanalytical Research**, **37**,  
705 277-296, <https://doi.org/10.1111/j.1751-908X.2012.00161.x>.

706  
707 **Lecumberri-Sanchez P., Bouabdellah M. and Zemri O. (2018)**  
708 Transport of rare earth elements by hydrocarbon-bearing brines: Implications for ore deposition and  
709 the use of REEs as fluid source tracers. **Chemical Geology**, **479**, 204-215,  
710 <https://doi.org/10.1016/j.chemgeo.2018.01.010>.

711  
712 **Lee K.-H., Shishido S., Kusachi I. and Motomizu S. (2000)**  
713 Determination of lanthanoids and yttrium in JGb2 and JR3 by inductively coupled plasma-mass  
714 spectrometry after cation-exchange pretreatment. **Geochemical Journal**, **34**, 383-393,  
715 <https://doi.org/10.2343/geochemj.34.383>.

716  
717 **Leisen M. (2011)**  
718 Analyse chimique des inclusions fluides par ablation laser couplée à l'ICP-MS et applications  
719 géochimiques. **PhD thesis, Nancy University**, 306 p, <https://www.theses.fr/2011NAN10149>.

720  
721 **Leisen M., Boiron M.-C., Richard A. and Dubessy J. (2012a)**  
722 Determination of Cl and Br concentrations in individual fluid inclusions by combining  
723 microthermometry and LA-ICPMS analysis: Implications for the origin of salinity in crustal fluids.  
724 **Chemical Geology**, **330–331**, 197-206, <https://doi.org/10.1016/j.chemgeo.2012.09.003>.

725  
726 **Leisen M., Dubessy J., Boiron M.-C. and Lach P. (2012b)**  
727 Improvement of the determination of element concentrations in quartz-hosted fluid inclusions by LA-  
728 ICP-MS and Pitzer thermodynamic modeling of ice melting temperature. **Geochimica et**  
729 **Cosmochimica Acta**, **90**, 110-125, <https://doi.org/10.1016/j.gca.2012.04.040>.

730  
731 **Liu Y., Chakhmouradian A.R., Hou Z., Song W. and Kynický J. (2018)**

732 Development of REE mineralization in the giant Maoniuping deposit (Sichuan, China): insights from  
733 mineralogy, fluid inclusions, and trace-element geochemistry. **Minerium Deposita**, **54**, 701-718,  
734 <https://doi.org/10.1007/s00126-018-0836-y>.

735

736 **Longerich H.P., Jackson S.E. and Gunther D. (1996)**

737 Laser ablation inductively coupled plasma mass spectrometric transient signal data acquisition and  
738 analyte concentration calculation. **Journal of Analytical Atomic Spectrometry**, **11**, 899-904,  
739 <https://doi.org/10.1039/JA9961100899>.

740

741 **Luais B., Telouk P. and Albarède F. (1997)**

742 Precise and accurate neodymium isotopic measurements by plasma-source mass spectrometry.  
743 **Geochimica et Cosmochimica Acta**, **61**, 4847-4854,  
744 [https://doi.org/10.1016/S0016-7037\(97\)00293-7](https://doi.org/10.1016/S0016-7037(97)00293-7).

745

746 **Luais B., Le Carlier de Veslud C., Géraud Y. and Gauthier-Lafaye F. (2009)**

747 Comparative behavior of Sr, Nd and Hf isotopic systems during fluid-related deformation at middle  
748 crust levels. **Geochimica et Cosmochimica Acta**, **73**, 2961-2977,  
749 <https://doi.org/10.1016/j.gca.2008.12.026>.

750

751 **Martin C., Duchêne S., Luais B., Goncalves P., Deloule E. and Fournier C. (2010)**

752 Behavior of trace elements in relation to Lu–Hf and Sm–Nd geochronometers during metamorphic  
753 dehydration–hydration in the HP domain of Vårdalsneset, Western Gneiss Region, Norway.  
754 **Contributions to Mineralogy and Petrology**, **159**, 437-458, [https://doi.org/10.1007/s00410-009-](https://doi.org/10.1007/s00410-009-0434-1)  
755 [0434-1](https://doi.org/10.1007/s00410-009-0434-1).

756

757 **Mercadier J., Cuney M., Lach P., Boiron M.-C., Bonhoure J., Richard A., Leisen M. and Kister**  
758 **P. (2011)**

759 Origin of uranium deposits revealed by their rare earth element signature. **Terra Nova**, **23**, 264-269,  
760 <https://doi.org/10.1111/j.1365-3121.2011.01008.x>.

761  
762 **Michaud C.F. (2011)**  
763 The role of cross-linking in ion exchange resins. **Water Conditioning and Purification Magazine**,  
764 <http://www.wcponline.com/2011/06/07/role-cross-linking-ion-exchange-resins/> (2011, June 7<sup>th</sup> ,  
765 accessed 3 April 2019).  
766  
767 **Mondillo N., Balassone G., Boni M., Chelle-Michou C., Cretella S., Mormone A., Putzolu F.,**  
768 **Santoro L., Scognamiglio G. and Tarallo M. (2019)**  
769 Rare Earth Elements (REE) in Al- and Fe-(Oxy)-hydroxides in bauxites of Provence and Languedoc  
770 (Southern France): implications for the potential recovery of REEs as by-products of bauxite mining.  
771 **Minerals**, **9**, 504, <http://dx.doi.org/10.3390/min9090504>.  
772  
773 **Nakamura K. and Chang Q. (2007)**  
774 Precise determination of ultra-low (sub-ng g<sup>-1</sup>) level rare earth elements in ultramafic rocks  
775 by quadrupole ICP-MS. **Geostandards and Geoanalytical Research**, **31**, 185-197,  
776 <https://doi.org/10.1111/j.1751-908X.2007.00859.x>.  
777  
778 **Paton C., Hellstrom J., Paul B., Woodhead J. and Hergt J. (2011)**  
779 Lolite: Freeware for the visualisation and processing of mass spectrometric data. **Journal of**  
780 **Analytical Atomic Spectrometry**, **26**, 2508, <https://doi.org/10.1039/c1ja10172b>.  
781  
782 **Pyle J.M., Spear F.S., Rudnik R.L. and McDonough W.F. (2001)**  
783 Monazite-xenotime-garnet equilibrium in metapelites and a new monazite-garnet thermometer.  
784 **Journal of Petrology**, **42**, 2083-2107, <https://doi.org/10.1093/petrology/42.11.2083>.  
785  
786 **Richard A., Rozsypal C., Mercadier J., Banks D. A., Cuney M., Boiron M.-C. and Cathelineau**  
787 **M., (2012)**  
788 Giant uranium deposits formed from exceptionally uranium-rich acidic brines. **Nature Geoscience**, **5**,  
789 142-146, <https://doi.org/10.1038/NGEO1338>.

790

791 **Roedder E. (1984)**

792 Fluid inclusions. In: **Ribbe P.H. (ed.), Reviews in Mineralogy, 12. Mineralogical Society of**

793 **America**, 644pp.

794

795 **Salvi S. and Williams-Jones A.E. (2006)**

796 Alteration, HFSE mineralisation and hydrocarbon formation in peralkaline igneous systems: insights

797 from the Strange Lake Pluton, Canada. **Lithos**, **91**, 19-34,

798 <https://doi.org/10.1016/j.lithos.2006.03.040>.

799

800 **Schlegel T.U., Wagner T. and Fusswinkel T. (2020)**

801 Fluorite as indicator mineral in iron oxide-copper-gold systems: explaining the IOCG deposit

802 diversity. **Chemical Geology**, **548**, 119674, <https://doi.org/10.1016/j.chemgeo.2020.119674>.

803

804 **Schmidt K., Garbe-Schönberg D., Bau M. and Koschinsky A. (2010)**

805 Rare earth element distribution in 400°C hot hydrothermal fluids from 5°S, MAR: The role of

806 anhydrite in controlling highly variable distribution patterns. **Geochimica et Cosmochimica Acta**,

807 **74**, 4058-4077, <https://doi.org/10.1016/j.gca.2010.04.007>.

808

809 **Seward T.M., Williams-Jones A.E. and Migdisov A.A. (2014)**

810 The chemistry of metal transport and deposition by ore-forming hydrothermal fluids. In: Holland H.D.

811 and Turekian K.K. (eds.), **Treatise on Geochemistry (Second Edition), Geochemistry of Mineral**

812 **Deposits, Elsevier (London)**, **13**, 29-57, <https://doi.org/10.1016/B978-0-08-095975-7.01102-5>.

813

814 **Sindern S. (2017)**

815 Analysis of Rare Earth Elements in Rock and Mineral Samples by ICP-MS and LA-ICP-MS. **Physical**

816 **Sciences Reviews**, **2(2)**, 20160066, <https://doi.org/10.1515/psr-2016-0066>

817

818 **Smith Y.R., Kumar P. and McLennan J.D. (2017)**

819 On the extraction of Rare Earth Elements from geothermal brines. **Resources**, **6(3)**, 39,  
820 <https://doi.org/10.3390/resources6030039>.

821

822 **Steinmann M., Stille P., Mengel K. and Kiefel B. (2001)**

823 Trace element and isotopic evidence for REE migration and fractionation in salts next to a basalt  
824 dyke. **Applied Geochemistry**, **16**, 351-361, [https://doi.org/10.1016/S0883-2927\(00\)00039-1](https://doi.org/10.1016/S0883-2927(00)00039-1).

825

826 **Tanaka T. and Musada A. (1982)**

827 The La–Ce geochronometer: a new dating method. **Nature**, **300**, 515-518,  
828 <https://doi.org/10.1038/300515a0>.

829

830 **Thompson R.L., Bank T., Montross S., Roth E., Howard B., Verba C. and Granite E. (2018)**

831 Analysis of rare earth elements in coal fly ash using laser ablation inductively coupled plasma mass  
832 spectrometry and scanning electron microscopy. **Spectrochimica Acta Part B: Atomic**  
833 **Spectroscopy**, **143**, 1-11, <https://doi.org/10.1016/j.sab.2018.02.009>.

834

835 **Truche L., Bazarkina E.F., Berger G., Caumon M.-C., Bessaque G. and Dubessy J. (2016)**

836 Direct measurement of CO<sub>2</sub> solubility and pH in NaCl hydrothermal solutions by combining in-situ  
837 potentiometry and Raman spectroscopy up to 280°C and 150 bar. **Geochimica et Cosmochimica**  
838 **Acta**, **177**, 238-253, <https://doi.org/10.1016/j.gca.2015.12.033>.

839

840 **Ulrich M., Bureau S., Chauvel C. and Picard C. (2012)**

841 Accurate measurement of rare earth elements by ICP-MS after ion-exchange separation: application  
842 to ultra-depleted samples. **Geostandards and Geoanalytical Research**, **36**, 7-20,  
843 <https://doi.org/10.1111/j.1751-908X.2011.00116.x>.

844

845 **Vasyukova O.V. and Williams-Jones A.E. (2018)**

846 Direct measurement of metal concentrations in fluid inclusions, a tale of hydrothermal alteration and  
847 REE ore formation from Strange Lake, Canada. **Chemical Geology**, **483**, 385-396,  
848 <https://doi.org/10.1016/j.chemgeo.2018.03.003>.

849

850 **Velásquez G., Borisova, A. Y., Salvi, S. and Béziat, D. (2012)**

851 In Situ Determination of Au and Cu in Natural Pyrite by Near-Infrared Femtosecond Laser Ablation-  
852 Inductively Coupled Plasma-Quadrupole Mass Spectrometry: No Evidence for Matrix Effects.

853 **Geostandards and Geoanalytical Research**, **36**, 315–324, <https://doi.org/10.1111/j.1751-908x.2012.00152.x>.

855

856 **Willie S.N. and Sturgeon R.E. (2001)**

857 Determination of transition and rare earth elements in seawater by flow injection inductively coupled  
858 plasma time-of-flight mass spectrometry. **Spectrochimica Acta Part B: Atomic Spectroscopy**, **56**,  
859 1707-1716, [https://doi.org/10.1016/S0584-8547\(01\)00263-4](https://doi.org/10.1016/S0584-8547(01)00263-4).

860

861 **Wood S.A. (1990)**

862 The aqueous geochemistry of the rare-earth elements and yttrium: 2. Theoretical predictions of  
863 speciation in hydrothermal solutions to 350°C at saturation water vapor pressure. **Chemical**  
864 **Geology**, **88**, 99-125, [https://doi.org/10.1016/0009-2541\(90\)90106-H](https://doi.org/10.1016/0009-2541(90)90106-H).

865

866 **Workman R.K. and Hart S.R. (2005)**

867 Major and trace element composition of the depleted MORB mantle (DMM). **Earth and Planetary**  
868 **Science Letters**, **231**, 53–72, <https://doi.org/10.1016/j.epsl.2004.12.005>.

869

870 **Zhu Y., Umemura T., Haraguchi H., Inagaki K. and Chiba K. (2009)**

871 Determination of REEs in seawater by ICP-MS after on-line preconcentration using a syringe-driven  
872 chelating column. **Talanta**, **78**, 891-895, <https://doi.org/10.1016/j.talanta.2008.12.072>.

873

## Tables

874

875 **Table 1.** Summary of the experiments with the REE oxides conducted in this study.

Run No	Initial composition, m – mol kg <sup>-1</sup> solution	Temperature, °C	Pressure, bar	Calculated pH <sub>TP</sub>	Total duration of experiment, days
2	Na <sub>2</sub> CO <sub>3</sub> 0.55 m	100	19-24	10.3	15
		150	18-22	9.9	
		200	23-25	9.7	
		250	40-42	9.6	
3	NaHCO <sub>3</sub> 0.63 m	100	22-35	7.6	17
		150	32-35	7.6	
		200	66-70	7.8	
		250	140-150	8.0	

876

877 **Table 2.** Instrumental operating parameters for ICP-MS.

ICP-MS model	X-Series 2 ThermoScientific
Type	Quadrupole
RF Power	1400W
Cool gas flow rate	13.5 l min <sup>-1</sup> Ar
Auxiliary gas flow rate	0.82 l min <sup>-1</sup> Ar
Sample gas flow rate	0.97 l min <sup>-1</sup> Ar
CeO/Ce	<0.03
Ba <sup>++</sup> /Ba	<0.035
Nebuliser	Microflow PFA
Spray chamber	PC <sup>3</sup> ESI Peltier Chiller, cooled to 2°C
Torch	Quartz glass torch
Sample Cone	Ni 4450
Skimmer Cone	Ni PS8R
Detector mode	Dual (pulse and analogue counting)
Dwell time / mass	Variable (10-15 ms)
Mass resolution	Standard
Solution uptake	peristaltic pump 12 rpm
Acquisition Mode	Peak Jumping
Number of sweeps	55
Channels	5
Number of repeats	3
Calibration	Indium as internal standard with on-line injection Standard solution control every five measurements
Isotopes	<sup>89</sup> Y, <sup>139</sup> La, <sup>140</sup> Ce, <sup>141</sup> Pr, <sup>143</sup> Nd, <sup>146</sup> Nd, <sup>147</sup> Sm, <sup>149</sup> Sm, <sup>151</sup> Eu, <sup>153</sup> Eu, <sup>157</sup> Gd, <sup>159</sup> Tb, <sup>161</sup> Dy, <sup>163</sup> Dy, <sup>165</sup> Ho, <sup>166</sup> Er, <sup>167</sup> Er, <sup>169</sup> Tm, <sup>171</sup> Yb, <sup>172</sup> Yb, <sup>175</sup> Lu

878

879 **Table 3.** The detection (DL) and quantification (QL) limits for the ICP-MS analyses, in pg g<sup>-1</sup>.

	<sup>89</sup> Y	<sup>139</sup> La	<sup>140</sup> Ce	<sup>141</sup> Pr	<sup>143</sup> Nd	<sup>146</sup> Nd	<sup>147</sup> Sm	<sup>149</sup> Sm	<sup>151</sup> Eu	<sup>153</sup> Eu	<sup>157</sup> Gd
DL, 3σ	21	4.5	0.6	1.0	4.7	1.9	1.7	28	0.6	0.6	1.2
QL, 10σ	37	11.4	1.3	1.8	9.6	4.5	3.6	43	1.5	1.3	2.8
	<sup>159</sup> Tb	<sup>161</sup> Dy	<sup>163</sup> Dy	<sup>165</sup> Ho	<sup>166</sup> Er	<sup>167</sup> Er	<sup>169</sup> Tm	<sup>171</sup> Yb	<sup>172</sup> Yb	<sup>175</sup> Lu	
DL, 3σ	0.21	0.9	0.6	0.12	0.15	1.5	0.16	0.9	0.7	0.08	
QL, 10σ	0.48	1.8	1.3	0.28	0.38	2.9	0.36	2.2	1.8	0.21	

880

881 **Table 4.** Instrumental operating parameters for LA-ICP-MS.

Laser type	GeoLas Excimer
Wavelength	193 nm
Laser frequency	5Hz
Fluence	7 J cm <sup>-2</sup>
Ablation cell	Internal diameter 5.5 cm, useful volume 24 cm <sup>3</sup>
Ablation spot size	60 μm
ICP-MS model	Agilent 7500cs
Type	Quadrupole
RF Power	1550W
Carrier gas flow rate	0.92 l min <sup>-1</sup> Ar
Vector gas flow rate	0.50 l min <sup>-1</sup> He
ThO/Th	<0.3
Th/U	0.98-1
Torch	Quartz glass torch
Sample Cone	Ni G1820-65238 made for Agilent by Spectron, Inc.
Skimmer Cone	Ni G3270-65024 for 7500ce/cx, Agilent Technologies
Sampling depth	5 mm
Detector mode	Dual (pulse and analogue counting)
Dwell time / mass	depending on the mass, see text
Background	30 s
Acquisition time	40 s (200 pulses)
Total time (1 analysis)	100 s
Number of repeats	6-7
Calibration	Calibrator (NIST SRM 610,), internal ( <sup>23</sup> Na)
Isotopes	<sup>23</sup> Na, <sup>89</sup> Y, <sup>139</sup> La, <sup>140</sup> Ce, <sup>141</sup> Pr, <sup>146</sup> Nd, <sup>147</sup> Sm, <sup>153</sup> Eu, <sup>157</sup> Gd, <sup>159</sup> Tb, <sup>163</sup> Dy, <sup>165</sup> Ho, <sup>166</sup> Er, <sup>169</sup> Tm, <sup>172</sup> Yb, <sup>175</sup> Lu

882

883 **Table 5.** Results of the cation-exchange resin column calibration, chemical yield (%).

Element	Y	La	Ce	Pr	Nd	Sm	Eu	Gd	Tb	Dy	Ho	Er	Tm	Yb	Lu	Mg	Ca	Na	K
Loaded, μg	43	20	20	20	20	20	20	20	20	20	20	20	20	20	20	6 879	18 810	32 608	69 246
Measured, μg	42	19	19	19	21	20	19	20	19	19	20	19	20	19	20	6 640	14 217	37 416	72 133
Yield, %	99	97	96	93	106	102	93	101	97	97	99	97	99	95	99	97	76	115	104

884

885 Chemical composition of solution used for calibration (prepared by weighting of certified standard solution  
 886 and salts): MgCl<sub>2</sub> 5.18 g l<sup>-1</sup>, CaCl<sub>2</sub> 10.01 g l<sup>-1</sup>, NaCl 15.93 g l<sup>-1</sup>, KCl 25.38 g l<sup>-1</sup>, lanthanides and Sc 3.85  
 887 mg l<sup>-1</sup>, Y 8.27 mg l<sup>-1</sup>. Volume: 5.2 ml.  
 888

889 **Table 6.** The REEs mass fractions in the blank solution (in pg g<sup>-1</sup>) and standard solutions (in ng g<sup>-1</sup>) after

890 the chemical treatment using the cation exchange resin AG<sup>®</sup> 50W-X8 (200-400 mesh) column.

Sample/REE	Y	La	Ce	Pr	Nd	Sm	Eu	Gd	Tb	Dy	Ho	Er	Tm	Yb	Lu	Sc*
Blank MQ-0, pg g <sup>-1</sup>	32	446	648	104	258	39	179	19	N/A	8	N/A	6	N/A	15	N/A	N/A
Blank MQ-1, pg g <sup>-1</sup>	51	426	474	61	234	44	106	48	5.2	32	7.6	26	5.2	19	5.3	591
Blank MQ-2, pg g <sup>-1</sup>	164	89	278	41	195	41	18	42	4.3	38	8.3	24	4.3	24	5.2	500
Blank salt-1, pg g <sup>-1</sup>	47	427	469	52	195	52	88	41	2.2	26	2.9	33	2.2	65	2.4	684
Blank salt-2, pg g <sup>-1</sup>	167	114	313	41	221	43	22	45	3.6	41	8.2	28	3.6	25	4.9	454
Standard 1, ng g <sup>-1</sup>	48	24	24	23	25	24	24	24	23	24	23	24	23	24	23	19
Standard 2, ng g <sup>-1</sup>	106	47	48	46	54	50	48	50	51	50	51	48	51	50	52	39

891

892 Blank MQ – REE-free Milli-Q solution treated like a sample;

893 Blank salt – REE-free 1 mol l<sup>-1</sup> NaCl solution treated like a sample;

894 Standard 1, reference mass fractions: REEs (lanthanides and Sc) 25.1 ng g<sup>-1</sup>, Y 50.9 ng g<sup>-1</sup>;

895 Standard 2, reference mass fractions: REEs (lanthanides and Sc) 51.0 ng g<sup>-1</sup>, Y 103.3 ng g<sup>-1</sup>.

896 N/A – not analyzed; \*Sc mass fractions were tentatively checked in blanks and standard solutions (yield 75-77%).

897

898 **Table 7.** Mean values of detection and quantification limits (DL and QL) acquired on standard solutions  
 899 during one LA-ICP-MS measurement session, in ng g<sup>-1</sup>.

	<sup>89</sup> Y	<sup>139</sup> La	<sup>140</sup> Ce	<sup>141</sup> Pr	<sup>143</sup> Nd	<sup>146</sup> Nd	<sup>147</sup> Sm	<sup>149</sup> Sm	<sup>151</sup> Eu	<sup>153</sup> Eu	<sup>157</sup> Gd
DL, 3σ	N/A	28	32	24	N/A	140	250	N/A	N/A	37	180
QL, 10σ	N/A	93	110	78	N/A	470	820	N/A	N/A	120	590

	<sup>159</sup> Tb	<sup>161</sup> Dy	<sup>163</sup> Dy	<sup>165</sup> Ho	<sup>166</sup> Er	<sup>167</sup> Er	<sup>169</sup> Tm	<sup>171</sup> Yb	<sup>172</sup> Yb	<sup>175</sup> Lu
DL, 3σ	49	N/A	75	31	55	N/A	24	N/A	88	23
QL, 10σ	160	N/A	250	100	182	N/A	80	N/A	293	78

\*N/A – not analyzed. Note, that for individual analyses, the best DL values rich ~10 ng g<sup>-1</sup>

900

901 **Table 8.** Fluid compositions of experimental samples in the H<sub>2</sub>O–NaHCO<sub>3</sub>–REEs system. LA-ICP-MS  
 902 data. Uncertainty (measurement repeatability) is expressed in terms of 3RSD.

Sample number	Na, mol/kg soln	ng g <sup>-1</sup>										
		Y	La	Ce	Pr	Nd	Sm	Eu	Gd	Dy	Er	Yb
3-0	0.63	6 845	-	3.6	43	421	1 827	4 447	17 695	2 460	325	1 523
3-1	0.62	15 525	-	5.7	29	147	958	2 982	10 080	9 500	960	4 160
3-2	0.65	53 945	-	12	132	228	706	3 412	6 315	37 360	13 865	55 650
3-3	0.65	59 250	-	16	466	505	1 747	3 300	7 400	43 345	32 965	97 750
3-4	0.63	55 510	-	12	240	344	1 472	3 323	7 665	40 905	33 605	101 750
3-5	0.65	19 135	-	8.4	419	142	490	980	2 245	8 850	26 300	155 000
3-6	0.67	14 380	-	bdl	287	90	361	852	2 059	8 620	21 620	104 067
3-7	0.67	14 270	-	bdl	186	66	296	814	1 896	9 180	17 635	86 100
3-8	0.60	N/A										
3-9	0.53	6 240	-	bdl	40	-	174	371	915	3 790	6 640	33 000
3-10	0.52	5 800	-	bdl	68	56	194	389	947	3 740	6 400	27 520
3-11	0.48	7 507	-	3.5	77	88	256	557	1 316	5 043	8 570	38 830
3-15	0.71	7 640	-	28	539	557	1 433	1 883	3 505	7 575	7 395	23 650
3RSD, %	±15	±25	-	±20	±20	±20	±25	±20	±25	±25	±25	±25

903

904 “bdl” – below detection limit; N/A – not analyzed. The samples N 3-12, 3-13, and 3-14 were not analyzed

905 because of the low concentration of sodium that was used as an internal standard for LA-ICP-MS. The

906 results of measurements with an unexploitable signal during laser ablation are not reported (-).

907

908

909 **Table 9.** Fluid composition of experimental samples in the H<sub>2</sub>O–NaHCO<sub>3</sub>–REEs system. ICP-MS after

910 ion-exchange resin Na-isolation. Uncertainty (measurement repeatability) is expressed in terms of 3RSD.

Sample number	Na, mol/kg soln	ng g <sup>-1</sup>										
		Y	La	Ce	Pr	Nd	Sm	Eu	Gd	Dy	Er	Yb
3-0	0.63	4 760	16	13	31	345	1 391	3 472	11 530	1 902	257	1 297
3-1	0.62	11 199	32	48	28	150	890	2 758	7 073	8 059	841	3 620
3-2	0.65	41 722	31	22	136	216	669	3 241	4 630	32 623	12 856	49 461
3-3	0.65	43 725	121	26	448	479	1 560	3 038	5 479	36 748	29 437	82 370
3-4	0.63	41 003	36	20	212	298	1 203	2 794	5 416	33 000	28 155	80 257
3-5	0.65	15 180	65	11	397	136	434	895	1 653	8 012	22 954	131 423
3-6	0.67	12 174	57	12	270	99	342	816	1 479	7 423	18 559	86 114
3-7	0.67	11 972	38	10	182	69	279	750	1 350	7 660	14 707	68 387
3-8	0.60	11 665	36	10	200	80	414	863	1 650	7 576	12 558	58 247
3-9	0.53	6 168	16	9.5	42	41	164	337	671	3 091	5 697	26 684
3-10	0.52	5 913	26	11	78	58	192	395	745	3 225	5 560	22 027
3-11	0.48	6 803	27	13	80	93	240	518	901	3 800	6 527	28 166
3-12	0.0051	946	22	19	22	22	43	96	188	643	508	997
3-13	0.0004	1 415	51	12	85	66	185	384	778	1 668	791	1 174
3-14	0.0058	149	13	15	2.7	11	12	24	41	73	37	58
3-15	0.71	5 102	86	32	383	393	869	1 292	2 158	5 394	5 440	16 476
3RSD, %	±15	±20	±10	±10	±10	±10	±10	±10	±15	±15	±15	±15

911 **Table 10.** Fluid composition in the H<sub>2</sub>O–Na<sub>2</sub>CO<sub>3</sub>–REEs system. LA-ICP-MS data. Uncertainty  
 912 (measurement repeatability) is expressed in terms of 3RSD.

Sample name	Na, mol/kg soln	ng g <sup>-1</sup>										
		Y	La	Ce	Pr	Nd	Sm	Eu	Gd	Dy	Er	Yb
2-0	1.1	119 733	7 715	387	2 603	2 215	4 060	325	136 400	73 300	13 970	6 020
2-1	1.2	183 133	4 425	312	1 813	2 907	17 237	1 625	207 333	81 400	16 260	5 430
2-2	1.2	199 133	1 808	267	1 064	2 328	15 307	1 587	181 533	76 000	15 573	5 447
2-3	1.2	230 150	1 384	211	861	1 980	13 045	1 371	160 650	78 700	16 915	5 850
2-4	1.2	126 200	311	14	208	430	2 085	211	36 900	69 000	90 900	86 300
2-5	1.2	36 570	481	11	567	1 705	4 519	100	16 165	21 800	36 825	39 470
2-6	1.2	19 700	-	bdl	360	-	7 300	-	10 710	10 450	21 400	22 400
2-7	1.2	33 495	770	12	783	1 437	9 050	157	19 250	20 260	35 435	44 425
2-8	1.1	29 390	723	11	943	1 520	6 240	157	16 695	17 925	32 765	47 335
2-9	1.2	24 770	450	7.4	1 012	1 143	3 358	101	10 060	13 715	30 015	52 100
2-10	1.2	24 430	-	bdl	608	-	-	-	6 740	10 870	31 400	56 200
2-11	1.2	11 800	-	bdl	214	175	384	30	1 383	4 050	13 945	26 700
2-12	0.7	4 865	-	bdl	125	128	446	24	1 515	1 949	3 620	4 435
2-13	1.3	14 910	-	bdl	32	86	390	81	1 625	5 305	12 115	12 445
3RSD, %	±15	±25	±45	±20	±20	±20	±25	±20	±25	±25	±25	±25

913 The results of measurements with an unstable signal during the laser ablation are not reported (-).

914 **Table 11.** Fluid composition in the H<sub>2</sub>O–Na<sub>2</sub>CO<sub>3</sub>–REEs system. ICP-MS after ion-exchange resin Na-  
 915 isolation. Uncertainty (measurement repeatability) is expressed in terms of 3RSD.

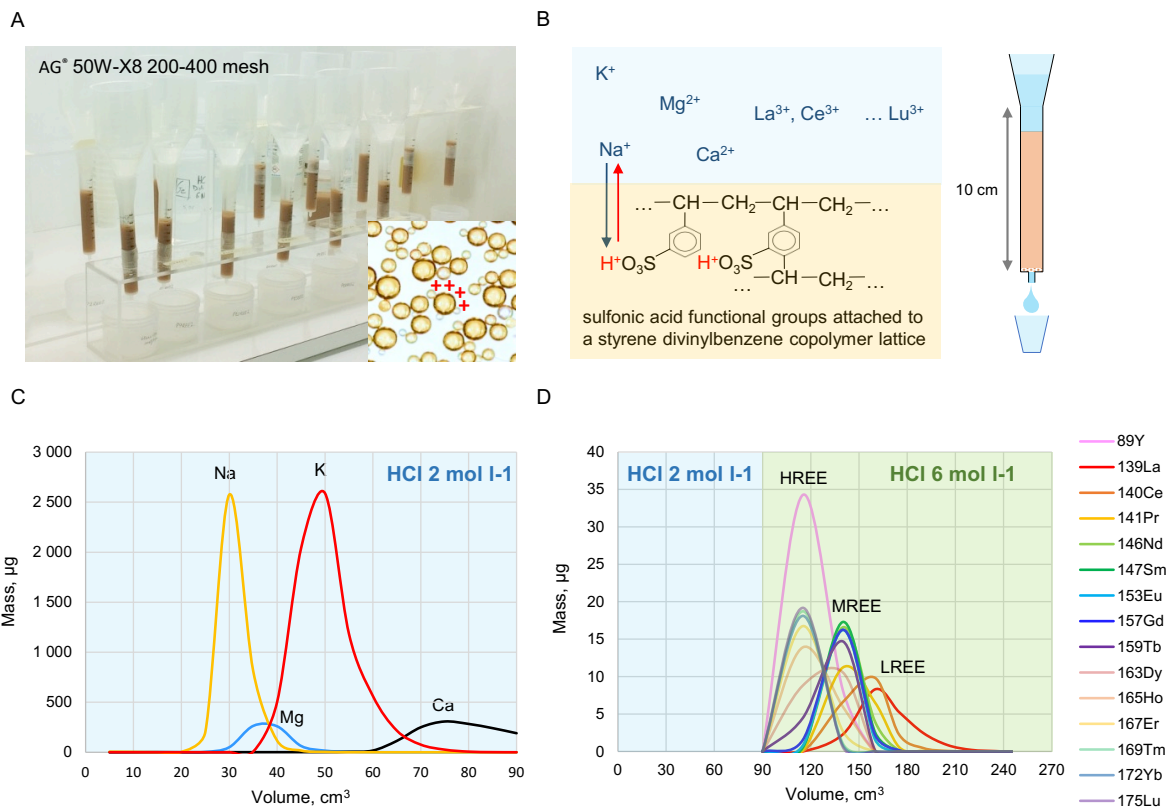
Sample name	Na, mol/kg soln	ng g <sup>-1</sup>										
		Y	La	Ce	Pr	Nd	Sm	Eu	Gd	Dy	Er	Yb
2-0	1.1	88 822	5 354	293	2 035	1 527	2 574	262	86 202	52 391	10 635	5 649
2-1	1.2	146 901	2 649	268	1 627	2 287	13 812	1 329	154 630	63 625	13 355	6 708
2-2	1.2	159 758	1 431	223	940	1 800	11 543	1 277	129 638	55 862	12 359	6 033
2-3	1.2	175 187	1 067	173	705	1 471	9 590	1 061	108 748	55 473	12 923	5 876
2-4	1.2	111 903	221	16	168	365	1 690	172	26 350	55 531	74 528	65 916
2-5	1.2	30 144	391	11	548	1 383	3 773	87	13 543	18 363	29 911	30 458
2-6	1.2	20 157	269	12	362	593	7 712	85	10 900	12 370	24 360	27 326
2-7	1.2	25 312	492	11	685	1 137	7 097	135	15 367	16 468	27 925	32 613
2-8	1.1	21 505	430	9.4	800	1 125	4 576	123	12 594	13 506	25 760	32 363
2-9	1.2	19 782	322	6.6	939	893	2 623	87	7 919	11 283	25 041	37 734
2-10	1.2	19 700	128	5.3	559	659	1 712	67	5 424	9 446	26 070	42 697
2-11	1.2	11 772	45	9.2	202	155	376	37	1 068	4 341	15 432	29 245
2-12	0.7	3 496	66	6.6	87	90	301	18	1 009	1 277	2 500	2 915
2-13	1.3	16 478	6.2	8.5	29	78	370	68	1 360	5 986	13 694	13 121
3RSD, %	±15	±20	±10	±10	±10	±10	±10	±10	±15	±15	±15	±15

916

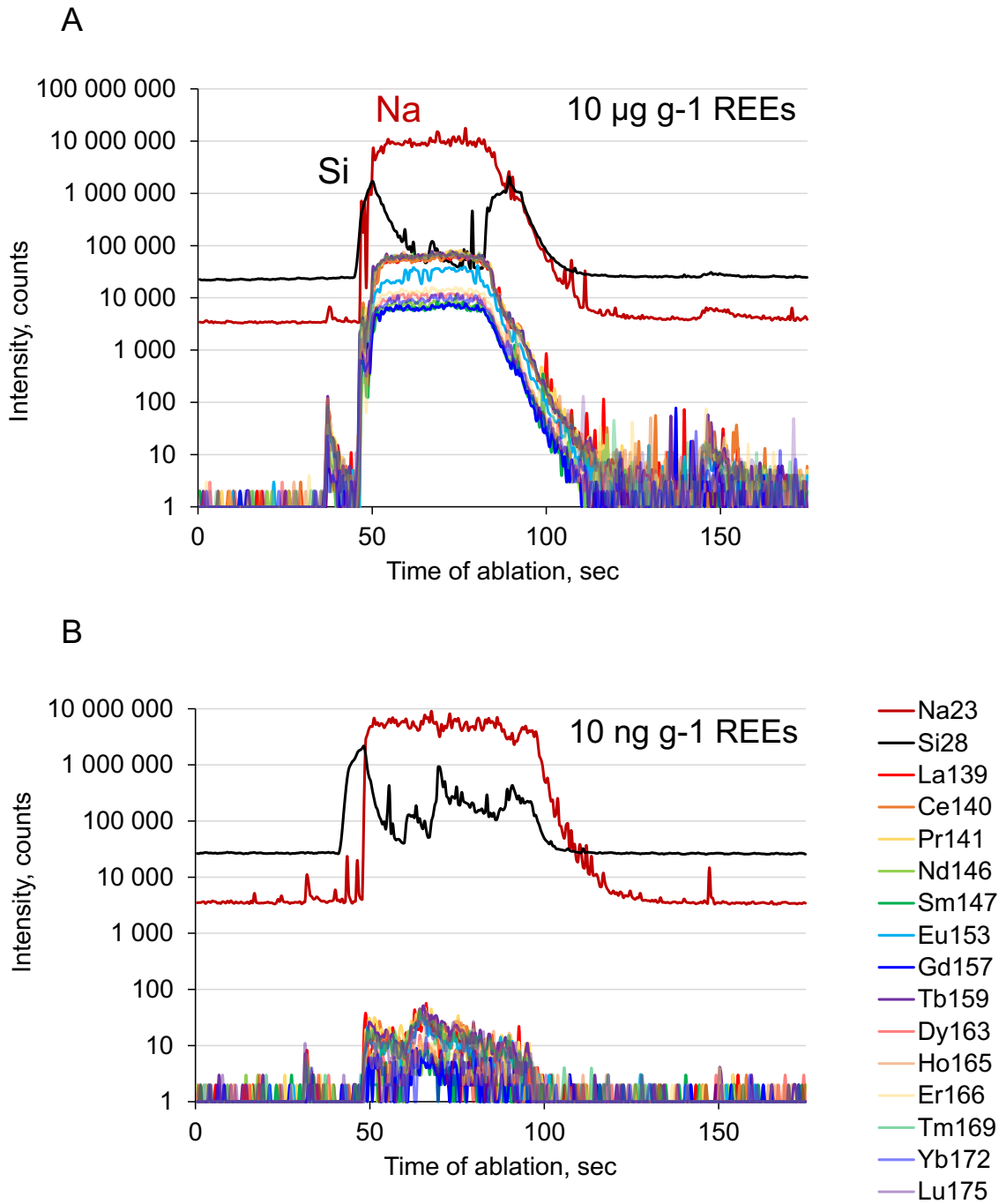
917 **Table 12.** Quantitative estimation of matrix effects observed on solutions during LA-ICP-MS.

Matrix effect, %	Matrix salt	La	Ce	Pr	Nd	Sm	Eu	Gd	Dy	Er	Yb
Underestimated vs prepared	NaCl 3.0 mol l <sup>-1</sup> pH = 5.5	4	13	17	3	2	26	6	36	41	30
Overestimated vs pn-ICP-MS	NaNO <sub>3</sub> 0.06-0.11 mol l <sup>-1</sup> pH = 1.0	47	22	18	30	26	16	41	30	19	22

918



920  
 921 **Fig. 1.** a) Photo of columns loaded with the cation exchange resin; b) schematic illustration of  
 922 the cation-exchange process in a column during elution with acid; c) elution of sodium,  
 923 magnesium, potassium and calcium-bearing matrix with HCl 2.0 mol l-1 solution; d) subsequent  
 924 removal of the REEs during elution with HCl 6.0 mol l-1.



925

926 **Fig. 2.** ICP-MS profiles of the REEs during the ablation of standard solutions in glass capillaries.

927

928

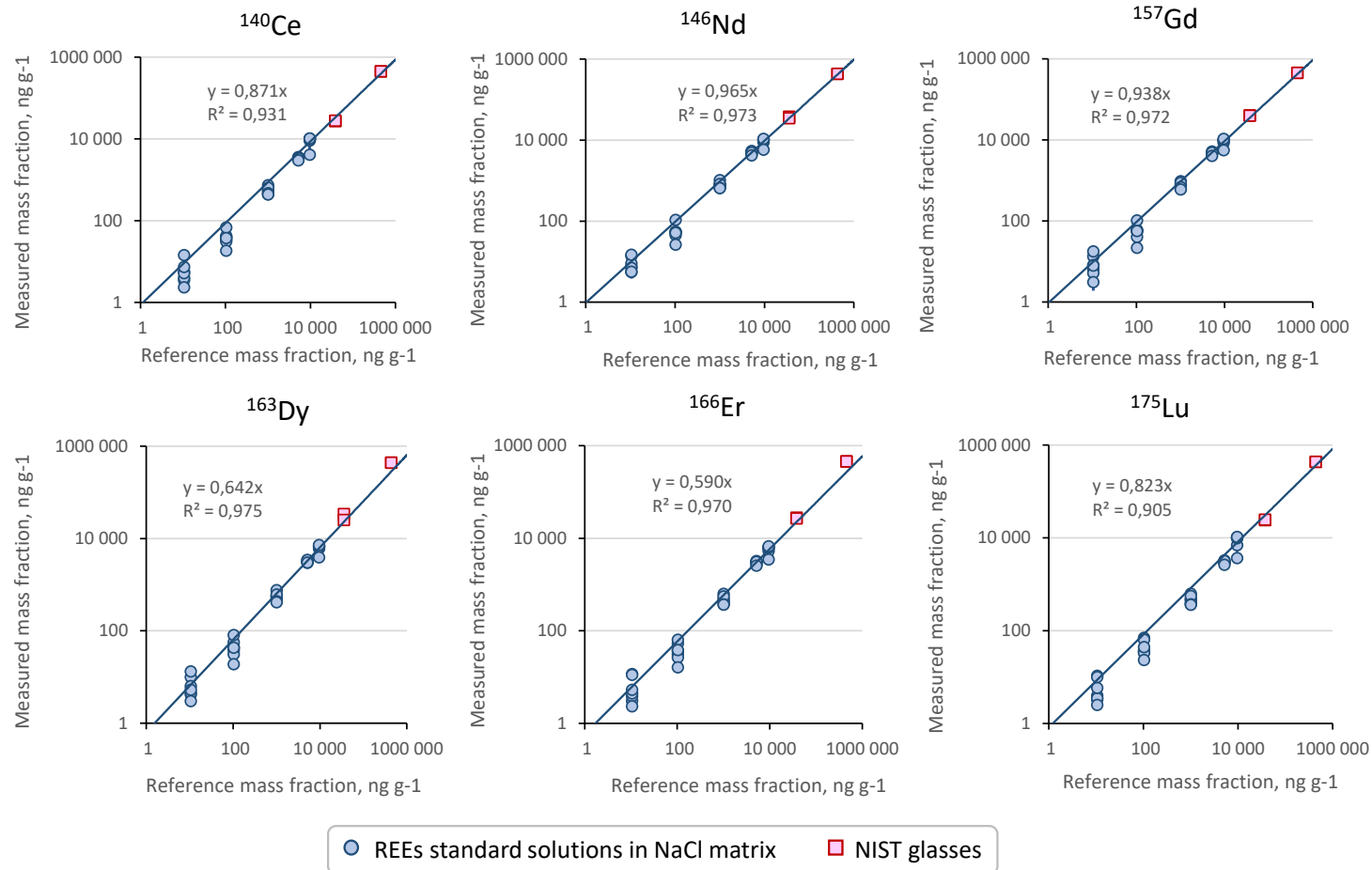


**Fig. 3.** REEs analyses of standard solutions obtained using LA-ICP-MS (for other REEs see [Electronic Supplementary Material](#)). Analytical uncertainties (2SD) are expressed in the symbols' sizes. Solid lines and corresponding equations represent the linear fits of the analytical results obtained for the prepared by weight standard solutions, whereas analyses of the NIST SRM glasses (610 and 612) used as calibrators are plotted for information.

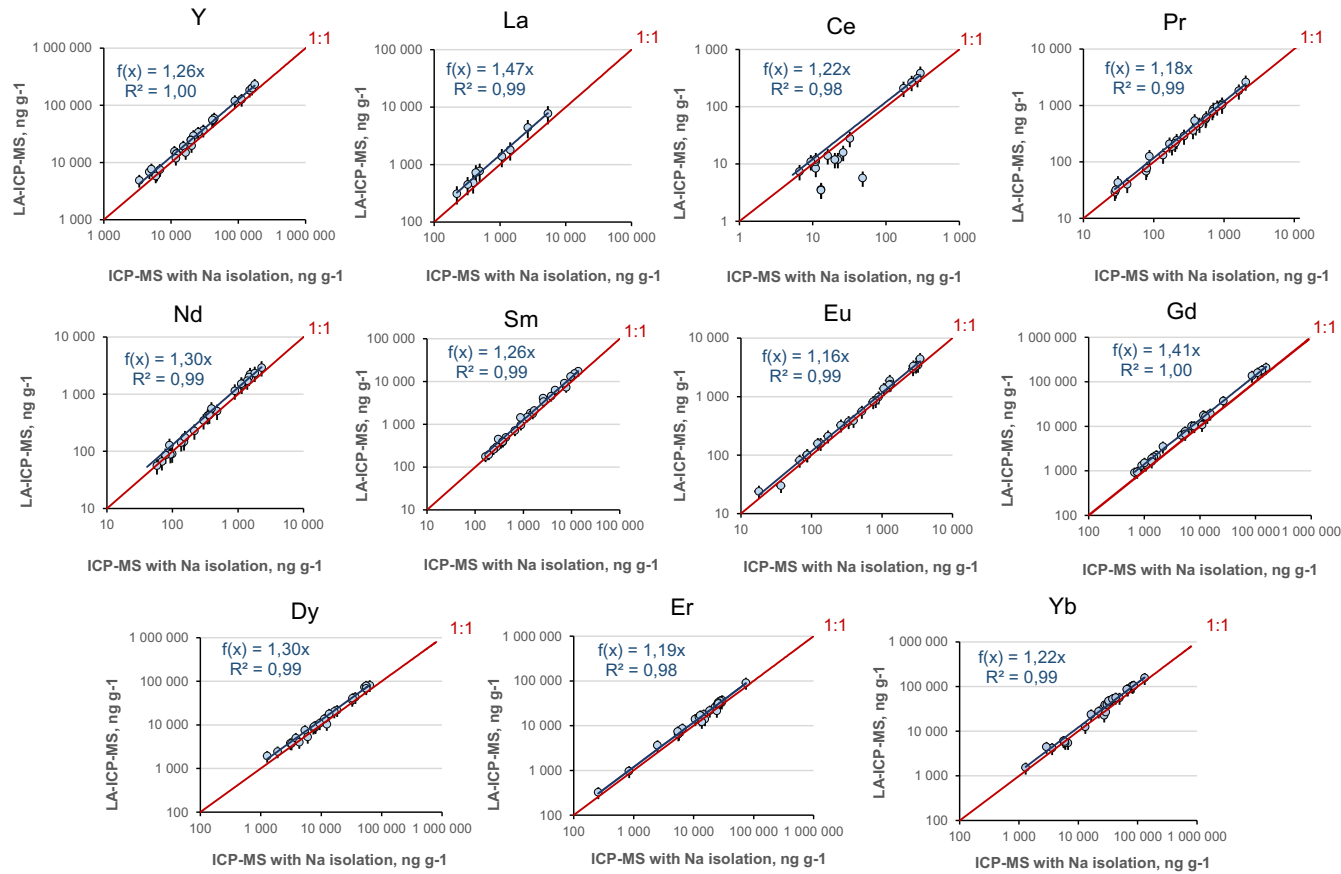


**Fig. 4.** Comparison of the mass fractions of the REEs in experimental solutions obtained using LA-ICP-MS and ICP-MS after sodium isolation (regression lines for elements are calculated taking into account the complete set of obtained analytical results, including the few outliers for Ce).